Journal of Cleaner Production 443 (2024) 141025

Contents lists available at ScienceDirect

Journal of Cleaner Production

journal homepage: www.elsevier.com/locate/jclepro

Biotechnological model for ubiquitous mixed petroleum- and bio-based plastics degradation and upcycling into bacterial nanocellulose

Jeovan A. Araujo [a,1,*], George Taxeidis [b,1], Everton Henrique Da Silva Pereira [a], Muhammad Azeem [a], Brana Pantelic [c], Sanja Jeremic [c], Marijana Ponjavic [c], Yuanyuan Chen [a], Marija Mojicevic [a,**], Jasmina Nikodinovic-Runic [c], Evangelos Topakas [b], Margaret Brennan Fournet [a]

[a] Centre for Polymer Sustainability, PRISM Research Institute, Technological University of the Shannon: Midlands Midwest, N37 HD68, Athlone, Ireland
[b] Industrial Biotechnology & Biocatalysis Group, Biotechnology Laboratory, School of Chemical Engineering, National Technical University of Athens, Iroon Polytechniou 9, 15772, Athens, Greece
[c] Institute of Molecular Genetics and Genetic Engineering, University of Belgrade, Vojvode Stepe 444a, 11000, Belgrade, Serbia

ARTICLE INFO

Handling Editor: Jian Zuo

Keywords:
Mixed plastic waste
Biodegradation
Enzymatic synergism
Plastic waste valorization
Bio-upcycling
Eco-polymers production

ABSTRACT

Ubiquitous post-consumer plastic waste is often physically mixed combining recalcitrant petroleum-based plastics with bioplastics, forming (petro-bio)plastic streams. Finding appropriate end-of-life (EoL) strategies for mixed (petro-bio)plastic waste is highly pertinent in achieving environmental protection, sustainability for plastic value chain industries including recyclers and government policy makers worldwide. The presence of bioplastic mixed in with polyethylene terephthalate (PET) or other petroleum-based plastic streams poses a substantial drawback to mechanical recycling and strongly impedes the development of sustainable EoL routes. Here, we present a model system for the sustainable management of mixed (petro-bio)plastic waste, demonstrating a biotechnological route through synergy-promoted enzymatic degradation of PET–representing petrochemical polyester plastic–mixed with thermoplastic starch (TPS)–as a model bioplastic. Leaf-branch compost cutinase (LCC^{ICCG}) and commercial amylase (AMY) deliver effective depolymerization of this mixed (petro-bio) plastic material, with subsequent bio-upcycling of the mixed waste stream into bacterial nanocellulose (BNC) by *Komagataeibacter medellinensis*. Compared to LCC^{ICCG} and AMY, the LCC^{ICCG}/AMY combined treatment synergistically produced a 2.6- and 4.4-fold increase in enzymatic decomposition at 70 °C in four days, respectively, yielding sugars and terephthalic acid (TPA) as the main depolymerization building blocks. Bio-upcycling of post-enzymatic degradation hydrolysates resulted in a high BNC yield of 3 g L^{-1} after 10 days. This work paves the way for sustainable management routes for challenging mixed recalcitrant plastic and bioplastic waste and prepares opportunities for its participation in the circular production of sustainable eco-polymers.

1. Introduction

Managing plastic pollution is undeniably one of the greatest societal challenges of the century. While the use of plastic spans simple daily needs to modern high-tech applications, nations are struggling to meet ambitious environmental targets set to manage an ever-increasing amount of plastic waste being generated every year (Borrelle et al., 2020). The traditional, highly linear end-of-life (EoL) treatment of plastics leads to incontrollable accumulation in the environment and failure to provide sustainable waste management for the safety of future generations and the planet. The current figures recorded for the distribution of post-use and waste plastics are alarming with accumulation in closed landfills or natural environments such as soils and oceans (79 %), incineration (12 %), or recycling (9 %) (Geyer et al., 2017; Wang et al., 2023). Polyethylene terephthalate (PET), one of the most produced recalcitrant thermoplastics worldwide and the highest produced polyester, is often considered the most circular of all plastics. Consequently, the extensive use of PET products, lack of appropriate technology and

* Corresponding author.
** Corresponding author.
E-mail addresses: a00204000@student.tus.ie, araujojeovan@gmail.com (J.A. Araujo), marija.mojicevic@tus.ie (M. Mojicevic).
[1] These authors contributed equally to this work.

https://doi.org/10.1016/j.jclepro.2024.141025
Received 25 October 2023; Received in revised form 24 January 2024; Accepted 28 January 2024
Available online 8 February 2024

waste management have already caused serious environmental issues and, with increasing production, this problem is expected to be exacerbated in the foreseeable future (Darko et al., 2023; Rochman et al., 2013). Due to their biodegradability, renewability and versatility, the plastic industry has seen a surge in market demand for bioplastics (Filho et al., 2021; Friedrich, 2021; Muhammad Shamsuddin, 2017), with global production capacity projected to increase by a 3.1-fold from 2021 to 2026 (European Bioplastics Conference, 2021). Consequently, traditional plastic waste streams are increasingly permeated by an array of bioplastics as the scale of their production increases (Ansink et al., 2022), forming mixed (petro-bio)plastic waste. In 2021, around 30 and 26 % of the global production capacity for biodegradable plastics were dedicated to produce polylactic acid (PLA) and starch blends, respectively (European Bioplastics Conference, 2021). Thermoplastic starch (TPS) has received increased attention because starch is an abundant, renewable biopolymer (Shafqat et al., 2020), and most importantly, TPS is fully biodegradable regardless of the environment as opposed to PLA being biodegradable only under industrially controlled conditions (Narancic et al., 2018). Nevertheless, the absence of established recycling streams for re-using bioplastics and recovering bioplastics from mixed (petro-bio)plastic streams is one of the current key challenges to sustainably transitioning from fossil- to bio-based plastics (Rosenboom et al., 2022). Post-consumer fossil- and bio-based plastics that contain a range of physically and chemically incompatible polymers from different sources, with a variety of limited to high potential end-of-use options, and an array of chemical structures, are disposed of jointly, thus contributing to the deterioration of the original properties of the conventional petroleum-based plastic waste recycling streams.

Concerning the EoL management of recalcitrant plastics, mixed plastic waste contains numerous challenging components, such as various synthetic plastics, non-plastic impurities, and bioplastics. As a first option for PET waste, mechanical recycling has emerged as an environmentally sustainable choice to enable the circularity of PET. However, the quality of the post-consumer PET recyclate must comply with specific standards. Expectedly, the success of mechanical recycling is severely limited by the low-quality of recyclate, resulting in degraded mechanical properties, and uneconomic costs (Schyns and Shaver, 2021). Alternatively, post-consumer PET can be chemically recycled via polymer breakdown into monomers, but the use of harmful chemicals and high temperatures makes it an environmentally hazardous and energy-intensive process (Thiounn and Smith, 2020). Furthermore, chemical recycling of mixed plastic waste result in complex mixtures of degradation products that require complicated additional separation steps to recover monomers for recycling (Sullivan et al., 2022). For these reasons, recyclers rely on costly and complex sorting techniques to separate plastics of interest from the mixed solid waste. Failure to deliver a proper separation of the mixed plastic waste will result in techno-economic difficulties for the recovery of materials, or most certainly in landfilling or incineration (Kulas et al., 2023). Existing advanced sorting techniques are unable to economically separate recycling into distinct streams in the case of bioplastic presence. In this context, a recent report has concluded that if the EU is to meet its carbon emission reduction targets, an EU-wide roll-out of mixed plastic waste sorting would need to be in place (Grant et al., 2023). Nonetheless, the report falls short to recommend how the exorbitant monetary cost of such imposition would be met by EU's member states. Thus, strategic development and implementation of sustainable pathways for mixed plastic waste is a pressing problem for current waste management practices.

To overcome these shortfalls, we propose a biotechnological route for the biodegradation of a mixed (petro-bio)plastic system, and further upcycling into new bio-based polymers (Fig. 1). Over the past years, microorganisms and enzymes have been considered as an emerging alternative for bioremediation of plastics to prevent improper waste disposal to the environment (Lee et al., 2023; Yang et al., 2023). On the one hand, composting is a decomposition process that results in useful compost for soil fertilization (Gioia et al., 2021), where the addition of selected microorganisms can significantly speed up the partial or

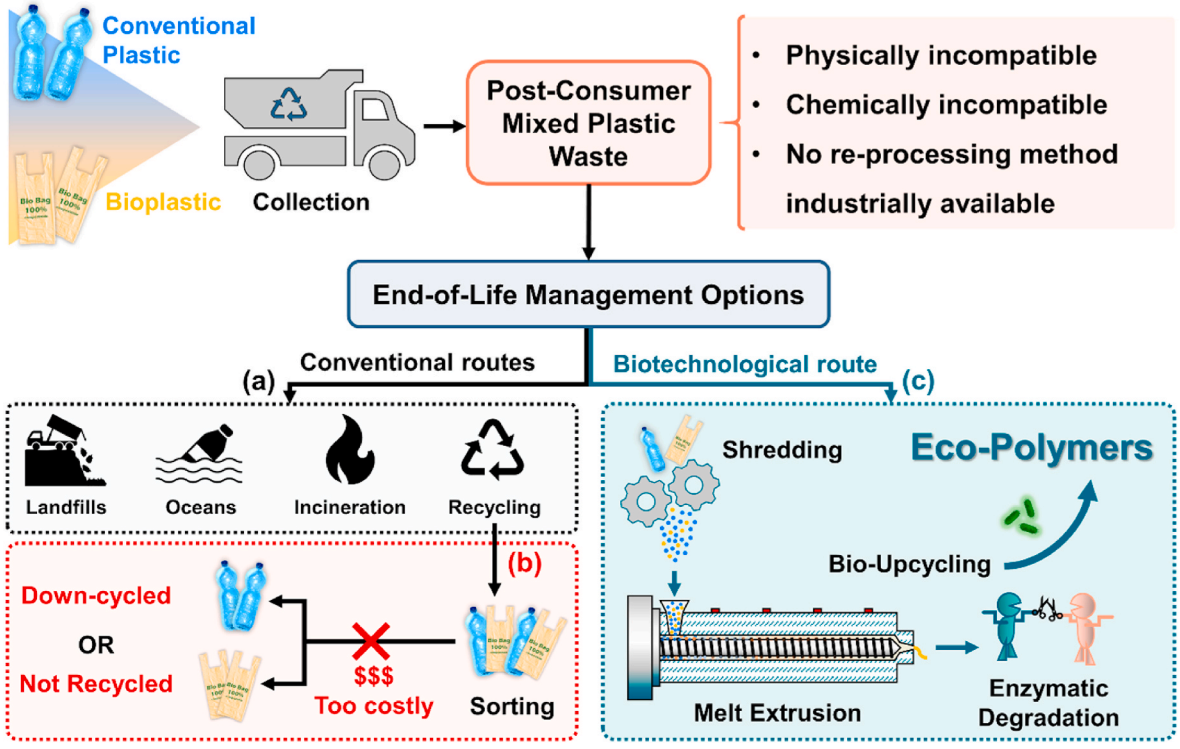

Fig. 1. End-of-life (EoL) management options for mixed (petro-bio)plastic waste: a) conventional destinations for mixed plastic waste; b) mechanical recycling of mixed plastic waste relies on expensive sorting techniques to provide partial recovery; and c) biotechnological approach proposed in this work to avoid expensive sorting and inappropriate disposal of mixed waste through tandem enzymatic degradation and bioconversion into eco-polymers.

complete disintegration process of biodegradable polymers (Quecholac-Piña et al., 2017). On the other hand, enzymatic degradation of PET still offers the eco-friendliest alternative for delivering PET circularity (Thomsen et al., 2022), as it requires mild reaction conditions, low energy and reagent consumption (Zhu et al., 2022). The PET backbone contains ester groups which are generally more biodegradable than C–C bonds. However, the substantial presence of aromatic terephthalate units in PET also decreases chain mobility which markedly restricts access to the hydrolysable ester bonds in the main chains. A number of studies was previously conducted to tune thermophysical properties of recalcitrant PET to make it amenable to biodegradation (Patel et al., 2023). The desired thermophysical characteristics of polyester substrates, such as high mobility of amorphous fraction, low glass transition temperature (T_g) and low crystallinity, directly influence the efficiency of enzymatic hydrolysis. For instance, higher amorphous fraction or lower crystallinity can accelerate enzyme penetration into crystalline lamellae, thereby increasing enzymatic depolymerization. Similarly, a low T_g provides enzymes with greater accessibility to molecular chains due to enhanced chain mobility of polymers which becomes more mobile above T_g (Patel et al., 2022). Wei et al. investigated biocatalytic efficiency of TfCut2 from *Thermobifida fusca* on postconsumer packaging and amorphous PET. It was concluded that amorphous regions of PET consist of both a rigid amorphous fraction and mobile amorphous fraction. Rigid amorphous fractions generally exhibit lower mobility of chains while mobile amorphous fraction provides chain mobility property to the total amorphous material. Results indicated that, compared to whole amorphous microstructures, the flexible mobile amorphous fraction is accessible to the polyester hydrolases (Wei et al., 2019a). A myriad of PET-hydrolyzing enzymes has been discovered and chemically characterized to date, including carboxylesterases, cutinases, and lipases (Tournier et al., 2023) that can cleave PET ester bonds resulting in bis(2-hydroxyethyl) terephthalic acid (BHET), mono-(2--hydroxyethyl) terephthalic acid (MHET), terephthalic acid (TPA), and ethylene glycol (EG) as degradation products. Thermostable cutinases such as LCC^{ICCG} and their homologues are the most efficient candidates due to their ability to operate at higher temperatures, closer to the T_g of PET, at which the mobility of the polymer chain is increased, leading to improved accessibility to the ester linkages between monomeric units (Soong et al., 2022). Interestingly, it has recently been reported that LCC^{ICCG} can also depolymerize biodegradable polyesters such as polycaprolactone (PCL), polybutylene succinate (PBS), polyhydroxybutyrate (PHB), and PLA (Makryniotis et al., 2023), making it a highly attractive enzyme for the treatment of mixed (petro-bio)plastic waste. Bio-upcycling is an important option to complement the EoL treatment of mixed plastic waste by revalorizing plastic debris. As opposed to harsh chemical treatments, enzymatic degradation is an advantageous approach that safely enables microorganisms to convert hydrolysates into added-value products (Kim et al., 2022). Among these products, bacterial nanocellulose (BNC) stands out as a material with immense potential for a wide range of applications due to its exceptional mechanical properties, making it a promising substitute for petroleum-based polymers (Navya et al., 2022). In spite of that, widespread use of BNC is restricted to excessive production costs (*ca.* 30 %) attributed to the culture medium (Jozala et al., 2016). Therefore, the use of post-degradation plastic debris as alternative cost-effective starting material for the production of BNC can be of great interest. Several bacterial genera including *Komagataeibacter*, *Agrobacterium*, *Aerobacter*, *Achromobacter*, *Rhizobium*, and *Pseudomonas* strains have been identified as BNC producers. Among these, *Komagataeibacter* is the most extensively studied and commonly used genus for BNC production. Besides BNC, biomaterials such as polyhydroxyalkanoates (PHAs) can potentially be obtained in similar process. Microbial production of these polymers was successfully implemented using TPS and PET monomers, separately (Gere and Czigany, 2018; Kourmentza et al., 2017).

In this work, we implemented a biotechnological model using different commercially available enzymes and the benchmark PET degrading LCC^{ICCG} to hydrolyze mixed (petro-bio)plastic materials (*i.e.* PET-TPS). Overall, this study presents a more sustainable EoL option for low-quality mixed (petro-bio)plastic (PET-TPS) waste streams using synergy-promoted enzymatic degradation, followed by a holistic biotransformation of the resulting by-products into BNC–a high-performance, multifunctional eco-polymer produced here adopting principles of a circular, bio-based economy for plastics.

2. Materials and methods

2.1. Materials

PET granules from Alpek Polyester UK Ltd. (Lazenby, UK) and thermoplastic potato starch (TPS) commercialized as Solanyl® C2002 by Rodenburg Biopolymers (Oosterhout, The Netherlands) were used to prepare a model mixed (petro-bio)plastic waste material. Commercial thermostable alpha amylase (AMY) (Liquozyme® SC DS) and glucoamylase (Spirizyme® Fuel) were obtained from Novozymes (Bagsværd, Denmark) and used as received. The gene encoding the quadruple variant of leaf branch compost cutinase (LCC^{ICCG}, variant F243I/D238C/S283C/Y127G) was provided by GenScript Biotech B.V. (Rijswijk, Netherlands). Ethanol (EtOH), isopropyl β-D-1-thiogalactopyranoside (IPTG), HPLC grade acetonitrile and sulfuric acid, tris hydrochloride (Tris-HCl), sodium chloride (NaCl), and phosphate-buffered saline (PBS) buffers, potassium hydroxide (KOH), and other chemicals used for preparation of bacterial growth medium, buffers, and degradation experiments were purchased from Sigma-Aldrich (Burlington, MA). Hestrin–Schramm (HS) (2 % glucose, 0.5 % yeast extract, 0.27 % disodium phosphate (Na_2HPO_4), and 0.15 % citric acid) was used as a control medium for the production of BNC by *Komagataeibacter medellinensis* ID13488 strain (Spanish Type Culture Collection, CECT 8140, Valencia, Spain). Ultrapure water was obtained from an Accu100 Ultrapure Water System (Fisher Scientific, Loughborough, UK).

2.2. Fabrication of the mixed PET-TPS films

PET-TPS materials were prepared from commercial resins as a model mixed (petro-bio)plastic waste. PET and TPS pellets were physically mixed and processed by hot-melt extrusion at different TPS weight ratios (wt.%), namely 5, 10, 30 and 40 %. Films were prepared using a benchtop Prism™ twin-screw extruder by Thermo Electron GmbH (Karlsruhe, Germany), with 16 mm diameter screws at a temperature profile of 270, 250, 200, 180, and 70 °C, respectively from feeding to die zone, with a screw speed of 60 rpm. The extruder was coupled with a 3-roll calendar system to form films. The thickness of all films, measured by Vernier caliper, was below 1 mm. The fabricated films were shredded into small pieces, frozen in liquid nitrogen, then milled into powdered samples by using an Ultra Centrifugal Mill ZM 200 from Retsch GmbH (Haan, Germany), operating at a rotor speed of 17,000 rpm. Resulting films and powdered samples were stored at room temperature until further use.

2.3. Characterization

2.3.1. Fourier transform infrared (FTIR) spectroscopy

The chemical changes of the PET-TPS samples were investigated by FTIR carried out on a PerkinElmer Spectrum One FTIR spectrometer (PerkinElmer Inc., Washington, USA) fitted with an attenuated total reflectance (ATR) sampling accessory. Spectra were recorded before and after mixed plastic degradation using a spectral resolution of 4 cm^{-1}, with 20 scans acquired for each spectrum (4000–650 cm^{-1}), and air as background at room temperature. From the FTIR results, it was possible to determine the carbonyl index value, *CI*, according to equation (1) (Fotopoulou and Karapanagioti, 2017).

$$CI = \frac{A_{1712\ cm^{-1}}}{A_{1408\ cm^{-1}}} \quad (1)$$

where $A_{1712\ cm^{-1}}$ corresponds to the intensity of band typical of carbonyl group, and $A_{1408\ cm^{-1}}$ is the intensity of deformation vibration of C–H band.

2.3.2. Differential scanning calorimetry (DSC)

The thermal behavior of the mixed plastic films was studied by DSC thermograms recorded using a DSC 2920 Modulated DSC (TA Instruments, New Castle, DE, USA) with a nitrogen flow rate of 30 mL min^{-1} to prevent oxidation. Calibration of the instrument was performed using indium as standard. All the samples were dried at 60 °C for 8 h prior to testing. Test specimens weighed 6–9 ± 0.01 mg and were measured on a Sartorius scale (MC 210 P; Goettingen, Germany). Measurements were carried out with samples crimped in non-perforated aluminum pans, against an empty pan as a reference, heated from 30 to 275 °C, at a 10 °C min^{-1} heating rate. The percentage degree of crystallinity (X_c) of each sample was calculated from the second heating cycle, according to equation (2):

$$X_c(\%) = \frac{\Delta H_m - \Delta H_c}{\Delta H_m^{\circ}} x\ 100 \quad (2)$$

where, ΔH_m is the apparent melt enthalpy of the test samples, ΔH_c is the cold crystallization, ΔH_m° is the melt enthalpy of 100 % crystalline PET, which has been reported as 140 J g^{-1} (Wunderlich, 1973).

2.3.3. Scanning electron microscopy (SEM)

The morphology of the mixed plastic films was analyzed by SEM images obtained using a Tescan Mira XMU (Tescan™, Brno, Czech Republic) in back scattered electron mode for surface analysis, with an accelerating voltage of 9 kV. Prior to analysis, tested samples were placed on individual aluminum stubs and sputtered with a thin layer of gold using a Baltec SCD 005 sputter for 110 s under vacuum at 0.1 mbar.

2.3.4. Tensile testing

The mechanical properties of the mixed plastic films were evaluated using a Lloyd Lr10k tensiometer (Ametek Ltd., West Sussex, UK) with a 2.5 kN load cell on standard test specimens. Each sample was measured using a Vernier caliper, and tests were recorded at room temperature, with a strain rate of 10 mm min^{-1}, initial gauge length of 20 mm, and using a pull-to-limit setup (stop at a strain of 30 %). The tensile tests were carried out in accordance with ASTM D882, recorded using Nexygen™ software, and a minimum of five replicates per sample were analyzed and presented as mean values ± standard deviation. From the stress-strain curves recorded, the tensile strength and Young's modulus of each sample were determined.

2.3.5. Statistical analysis

Paired *t*-test (two sample for means) significance method was used to test the means of mechanical properties of PET with and without the presence of bioplastic, being considered statistically significant when the probability value (p) was found to be $p \leq 0.05$, and tests were performed using the data analysis tools add-in feature on MS Excel Software (Microsoft Corporation, Redmond, WA, USA).

2.4. Biodegradation of the mixed PET-TPS materials

2.4.1. Model home composting bioaugmented with Bacillus sp. BPM12

Biodegradation of the studied mixed PET-TPS materials was first assessed by implementing a laboratory scale model home composting, using bioaugmented compost treated with a novel *Bacillus* sp. BPM12 strain (Pantelic et al., 2023) for 10 weeks at 37 °C, according to a previously described protocol (Pantelic et al., 2021) (Text S1, supplementary data).

2.4.2. Preparation of recombinant LCC enzyme

In order to examine the biodegradability of the mixed PET-TPS films, genes coding LCC^{ICCG} were synthesized following a known method (Tournier et al., 2020), codon optimized for expression in *E. coli*, and cloned in the expression vector pET26b(+) (GenScript Biotech, Rijswijk, Netherlands). The enzyme expression was performed in *E. coli* BL21 induced by 0.2 mM IPTG at 16 °C for 20 h, according to a previously described protocol (Dimarogona et al., 2015). After enzyme expression, the cells were harvested by centrifugation at 4000*g* for 15 min at 4 °C (Eppendorf Centrifuge 5417 R, Hamburg, Germany), and resuspended in 50 mM Tris-HCl, 300 mM NaCl pH = 8 buffer. Cell suspension was disrupted by sonication during four 1-min cycles (8 s pulses and 5 s pause) at 40 % amplitude using a 20 kHz high intensity (400 W) ultrasonic processor (VC 400, Sonic & Materials, Newtown, CT, USA). After cell lysis, the cell debris was removed by centrifugation at 20,000*g* for 30 min at 4 °C, and the liquid fraction was purified using an immobilized metal-ion (Co^{2+}) affinity chromatography (IMAC) (Nikolaivits et al., 2022). The purity of isolated enzymes was checked on SDS-PAGE electrophoresis (Bio-Rad, Hercules, CA, USA) (12.5 % poly-acrylamide) and protein concentration was determined by measuring the absorbance at 280 nm. The molar extinction coefficient used (LCC^{ICCG}: 28,836 M^{-1} cm^{-1}) was calculated by ProtParam tool from ExPASy (Gasteiger et al., 2005).

2.4.3. Enzymatic degradation study

PET-TPS film samples were rinsed with 70 % EtOH, air dried, weighted and inserted in glass flasks. The following enzyme preparations were used for degradation experiments: (1) LCC^{ICCG}; (2) AMY; and (3) LCC^{ICCG}/AMY. Degradation experiments with LCC^{ICCG} and AMY were performed using film samples hydrolyzed in 0.1 M phosphate buffer, pH = 7, under agitation (1200 rpm) in an Eppendorf Thermomixer Comfort (Hamburg, Germany). Typically, 10 mg of each sample was added to 1 mL of reaction medium, and enzymatic treatments were optimized by conducting reactions at three different temperatures, namely 30, 50 and 70 °C. All tests were carried out on a continuous base for a period of four days. Hydrolysis reaction was initiated by adding 0.12 μg of LCC^{ICCG} which had been dialyzed in Tris-HCl buffer, pH = 7. Moreover, 30 μg of AMY was also added to the reaction mixture to assess the combined effect of these enzymes on the degradation of mixed PET-TPS materials. This addition was also made in the case of PET, primarily for comparative purposes with the other tested materials. In control reactions, an equal amount of Tris-HCl buffer or deactivated AMY (boiled for 15 min) was added to the reaction mixture. After 24, 48, and 72 h, half of the initial amount of each enzyme was added to the reaction mixture to sustain the enzyme activity, thus mitigating enzyme issues related to thermal inactivation, and adsorption onto the material surface (Makryniotis et al., 2023). At the end of the reactions, the residual material was isolated by centrifugation, washed with ultrapure water, freeze-dried and its weight was measured. The reaction supernatant was analyzed by high-performance liquid chromatography (HPLC) and the dinitrosalicylic acid (DNS) colorimetric method to detect degradation products from the mixed PET-TPS plastic films.

2.4.4. Quantification of BHET, MHET, and TPA via HPLC analysis

Samples were prepared by adding 1 μL of 6 M HCl (50 % aqueous solution of concentrated HCl) to 1 mL of reaction supernatant, vortexed and centrifuged for 15 min at 12,000 rpm. The supernatant was filtered through 0.2 μm syringe filters. For the HPLC analysis, an UltiMate 3000 HPLC (Thermo Fisher Scientific, Waltham, USA) coupled with an Eurospher II 100-3 C18A 150 × 4.6 mm column (Knauer, Germany) was used. The mobile phase consisted of 20 % (v/v) acetonitrile and 80 % (v/v) 2.5 mM sulfuric acid in ultrapure water at a flow rate of 0.8 mL min^{-1} under isocratic conditions. Detection of reaction products was carried out using an ultraviolet–visible (UV–vis) detector at 241 nm and the total run time was set at 25 min. Quantification of TPA, MHET, and BHET was performed following the same HPLC protocol described above (Fig. S1, supplementary data).

2.4.5. Quantification of reducing sugars via DNS colorimetric method

The total amount of reducing sugars was quantified using the DNS colorimetric method. The DNS method was performed according to the traditional protocol (Miller, 1959), with modifications made to reduce the reaction volumes. Sugar levels were quantified at 540 nm using the SpectraMax® ABS Plus microplate reader (Molecular Devices, Sunnyvale, CA, USA), and data were processed using SoftMax® Pro 7 software (Molecular Devices, Sunnyvale, CA, USA). A calibration curve was constructed using glucose as a standard (Fig. S2, supplementary data).

2.4.6. Degree of synergism

Based on the detected concentration of degradation products from the mixed PET-TPS films, the degree of synergism (DS) between LCC^{ICCG} and AMY to degrade the different films was determined. The DS was calculated using equation (3):

$$DS = \frac{DP_{LCC/AMY}}{DP_{LCC} + DP_{AMY}} \quad (3)$$

where, $DP_{LCC/AMY}$ is the degradation products released by LCC^{ICCG}/AMY, DP_{LCC} is the degradation products released by LCC^{ICCG}, and DP_{AMY} is the degradation products released by AMY.

2.5. Bio-upcycling of PET-TPS degradation products

2.5.1. Scale-up of the enzymatic degradation

After enzymatic treatment was proven to be successful on examined materials, experiment was set up in larger volumes using 1 g of each PET-TPS powdered sample. Samples were treated in 50 mL of 0.1 M phosphate buffer, pH = 7, at 50 °C in a shaking incubator (200 rpm) for four days. More specifically, material hydrolysis was initiated after the addition of 1.2 μg of LCC^{ICCG} dialyzed in Tris-HCl buffer, as mentioned previously, while an equal amount of the enzyme was supplemented after 48 h. TPS liquefaction was accomplished by adding 300 μg of AMY, whereas in control reactions, an equal amount of Tris-HCl or deactivated AMY was added. After four days, 500 mg of glucoamylase was added to each of the reactions, and the reaction mixture was kept under the same conditions for an additional hour to ensure the total conversion of released reducing sugars into glucose, facilitating their quantification and subsequent valorization. Finally, the residual material was isolated by centrifugation, washed twice with ultrapure water, and freeze-dried before its weight was measured. The reaction supernatant was analyzed by HPLC and DNS methods to detect the released products after the mixed PET-TPS degradation according to the protocols aforementioned. Hydrolysates were kept for composition analysis, and further bio-upcycling into BNC.

2.5.2. Bacterial nanocellulose (BNC) production

Liquid residues obtained from the enzymatically degraded mixed PET-TPS materials were used as growing medium for the production of BNC by *Komagataeibacter medellinensis* ID13488. Typically, 2 mL of each liquid residue was poured into glass tubes, and pH was adjusted to 4.5 by using 0.05 mol L^{-1} HCl and NaOH solutions, then 10 % bacterial inoculum was added. Prior to inoculation, bacterial culture was rinsed with PBS buffer followed by centrifugation, to secure the removal of any additional carbon and energy sources from the production media. All samples were statically incubated at 28 °C for 10 days. HS medium was used as a positive control. After 10 days, the BNC obtained was treated with 5 % KOH, rinsed with distilled water until neutral pH was reached, air dried at 60 °C, and weighted. All BNC growth trials were performed in triplicates.

3. Results and discussion

In order to attain plastic circularity, this study proposes an alternative EoL management to prevent incineration or landfilling of lower-quality mixed plastics by demonstrating a biotechnological route to degrade mixed (petro-bio)plastic material (*i.e.* PET-TPS), and further bio-upcycle into high added value BNC. In our pursuit of a more sustainable option for such mixed (petro-bio)plastic waste, this work was divided into three main stages, as depicted in Fig. 2.

3.1. Fabrication and characterization of mixed (petro-bio)plastic films

In the first part of this work, we used TPS as a model bioplastic to simulate the problem of fossil-based PET recycling streams that are unrestrained mixed with bio-based plastics (Siddiqui et al., 2021). Hot-melt extrusion was used to compound PET and TPS at different weight ratios prior to enzymatic depolymerization, as presented in Table 1. Recently, Patel et al. have studied melt processing of PET as a pretreatment for enzymatic depolymerization of single plastic waste, while Åkesson et al. have suggested that even at 1 % contamination the highly dense hydroxyl groups present in TPS are chemically incompatible with the ester linkages of PET backbone (Åkesson et al., 2021; Patel et al., 2022). To verify the above claim, the effect of varying the TPS content mixed with PET in the extruded materials was evaluated in terms of changes in the films' chemical, thermal, and mechanical properties which were unveiled by FTIR, DSC, and tensile testing, respectively.

Chemical changes in the functional groups and fingerprint regions of the extruded mixed PET-TPS films (Fig. 3, top) were inspected by FTIR-ATR (Fig. 3, bottom). Characteristic bands of PET that were observed in the range from 3055 to 2850 cm^{-1} were assigned to aromatic and aliphatic –C–H bond stretching, at 1712 cm^{-1} was attributed to the stretching of the ester carbonyl group –C═O, and at 1244 and 1095 cm^{-1} were assigned to the C–O stretching and the methylene group vibrations, respectively (Chen et al., 2012). Also, the band at 871 cm^{-1} was indicative of aromatic ring C–H out-of-plane bending (Donelli et al., 2009), while the bands at 1370 and 1340 cm^{-1} were attributed to *gauche* and *trans* conformations of the CH_2 wagging vibrations. Moreover, change in the intensity of these two bands reveals the occurrence of an amorphous or semi-crystalline phase, so the ratio of these two bands indicates a change in the crystalline domains of PET (Sammon et al., 2000). As the amount of TPS present in PET increased from 0 to 40 %, a decrease of the 1340 cm^{-1}/1370 cm^{-1} absorbance ratio was clearly noted, which declined from 1.99 in the reference neat PET film to 1.11 in the mixed PET-TPS40 material. Therefore, it is suggested that the presence of TPS mixed in the PET stream has affected the close packing nature of the polyester crystalline phase and, consequently, promoted an amorphization process of the PET content. The spectrum of neat TPS film (Fig. S3, supplementary data) has been previously examined elsewhere in the literature (Araujo et al., 2021). In comparison to the spectrum of the neat PET (Fig. 3a, bottom), the spectra of the mixed PET-TPS films exhibited four distinct bands due to the reactive interactions between the two polymeric components. As it is clearly shown in the spectrum of the PET-TPS40 film (Fig. 3e, bottom), the presence of

Fig. 2. Schematic detailing the main stages of the proposed biotechnological route for the end-of-life (EoL) management of mixed plastic waste: a) preparation of a model mixed (petro-bio)plastic (PET-TPS) system; b) biodegradation of mixed (petro-bio)plastics resulting in low-cost starting materials; and c) bio-upcycling of low-cost waste-derived materials into new high-value eco-polymers.

Table 1
Composition by weight and thermo-mechanical properties of the fabricated mixed (petro-bio)plastic films.

Sample	PET (wt.%)	TPS (wt.%)	T_g (°C)	T_m (°C)	ΔH_m (J g^{-1})	X_c (%)	E (MPa)	σ (MPa)
PET	100		83.6	252.9	52.4	37.5	2239 ± 105	38 ± 5
PET-TPS5	95	5	79.2	246.9	49.0	35.0	2093 ± 215	21 ± 1
PET-TPS10	90	10	76.7	247.2	48.5	34.6	2028 ± 61	21 ± 2
PET-TPS30	70	30	54.2	248.4	45.2	32.3	1985 ± 135	19 ± 3
PET-TPS40	60	40	50.7	245.4	36.6	26.1	1628 ± 83	13 ± 2

T_g, glass transition temperature; T_m, melting temperature; ΔH_m, melting enthalpy; X_c, degree of crystallinity; E, Young's modulus; σ, tensile strength.

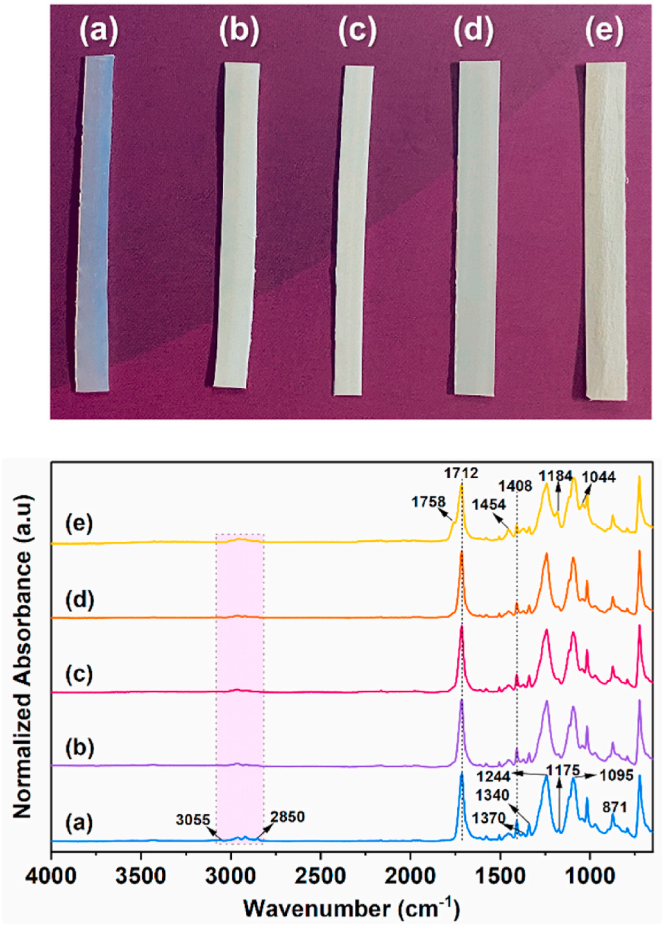

Fig. 3. Digital images (top) and FTIR spectra (bottom) of the studied mixed (petro-bio)plastic films: (a) neat PET, (b) PET-TPS5, (c) PET-TPS10, (d) PET-TPS30, and (e) PET-TPS40 films.

TPS is confirmed by the bands present at 1758 cm^{-1} that was assigned to the stretching of C═O group, at 1454 cm^{-1} which corresponded to C–H bending vibrations, and at 1184 and at 1044 cm^{-1} that were assigned to changes in the C–O and C–O–H stretching vibrations of TPS molecules (Bergel et al., 2018; Diop et al., 2011).

The thermal properties of the mixed (petro-bio)plastic films with varying bioplastic content were evaluated by DSC. The results obtained from the second heating step of the thermal analysis are shown in Table 1. The thermogram of the neat PET film showed its glass transition temperature (T_g) at about 84 °C, a characteristic endothermic melting peak (T_m) at almost 253 °C, and a resulting X_c = 37 %, which are in agreement with previous reports in the literature (Del Mar Castro López et al., 2014). When the amount of TPS bioplastic mixed in the PET material was increased, T_g and X_c were clearly reduced, confirming the decline in PET crystalline phase as previously indicated by the FTIR results. Particularly, T_g reduced to around 50 °C and X_c decreased to only 26 % in the PET material with the highest bioplastic content (*i.e.* PET-TPS40), respectively. In addition, a lower X_c was observed following the thermomechanical processing used prior to enzymatic degradation (Fig. S4, Table S1, supplementary data). PET monomeric units are linked by ester linkages resulting from the polymerization reaction between TPA and EG. X_c can be used to describe the level of mobility of the ester linkages that link PET monomeric units, which can be associated to a measure of the polymer segmental motion (Zekriardehani et al., 2017). Thus, the reduced X_c indicated lesser rigidity in the linkages, lowering the restriction in polymer chain motion. Furthermore, T_g is the temperature at which a transition from the glassy to the rubbery state occurs and, consequently, the mobility of the polymer chains is improved. Following the thermomechanical extrusion process, the decrease in T_g and X_c reported for the mixed PET-TPS films indicated that the ester linkages in PET became more accessible at lower temperatures. As a result, the increased mobility could enhance the activity of polyester hydrolases by allowing their access to the target ester linkages. Patel et al. have recently reported on the importance of thermally pretreating single plastic PET to enhance enzymatic depolymerization by promoting irreversible macromolecular changes caused by thermal and mechanical shear (Patel et al., 2022), therefore our findings indicate that a similar pretreatment concept could be used to advance the depolymerization of complex mixed PET streams using enzymes. In agreement with this decay of the thermal properties, Åkesson et al. recently investigated the effect of up to 5 wt% bioplastic content on the mechanical recycling of conventional plastics, and they reported suggestive decreases in the T_g and X_c values of PET (Åkesson et al., 2021). To gain more insights into the effect of bio-based polymers present in PET recycling streams, the mechanical properties of the fabricated films were assessed in terms of Young's modulus (E) and tensile strength (σ) (Text S6, supplementary data). In general terms, it is clear that the mixed (petro-bio)plastic with increased TPS content triggered the deterioration of mechanical properties, which is consistent with the decay of thermal properties previously presented, particularly the T_g and X_c, suggesting that such plastic streams would be unsuitable for mechanical recycling as an EoL option for the mixed (petro-bio)plastic waste.

3.2. Biodegradation of the fabricated mixed PET-TPS films

A recent study has isolated and identified a novel bacterium strain named *Bacillus subtilis* BPM12 that efficiently interacts with PET and can hydrolyze its intermediate compounds (Pantelic et al., 2023). Therefore, in the second stage of our study we first developed a model home composting system bioaugmented with *Bacillus* sp. BPM12 to evaluate the biodegradation of mixed PET-TPS materials, which were initially assessed in terms of biodegradation and further characterized by FTIR (Fig. S5, supplementary data) and SEM (Fig. S6, supplementary data) analysis, but decomposition was limited to only 3.4 and 4.1 % weight loss from nontreated and bioaugmented compost, respectively (Text S7, supplementary data), making home composting an unsuitable route for the biodegradation of the studied mixed (petro-bio)plastic system. A reasonable explanation is that home composting is a bioremediation process for plastic treatment that occurs under uncontrolled conditions–hence, degradation rates can be very unpredictable. A more interesting alternative to delve into treatment options for such mixed

(petro-bio)plastic streams following a thermomechanical extrusion pre-treatment could be industrial composting, however such assessment is out of the scope of this work. Conversely, various enzymes have also shown the ability to degrade PET, including natural or engineered esterases such as PETase (Yoshida et al., 2016), carboxylesterase (von Haugwitz et al., 2022), and cutinases (Sintawee et al., 2012; Tournier et al., 2020). Therefore, we turned our efforts to investigate the biodegradation of the mixed (petro-bio)plastic waste by exploring the biocatalytic potential of three different enzymatic systems (*i.e.* AMY, LCC^{ICCG}, and LCC^{ICCG}/AMY).

3.2.1. *Enzymatic hydrolysis of the mixed PET-TPS films*

To investigate the breakdown of the mixed PET-TPS samples, we selected LCC^{ICCG} and AMY as these enzymes show great performance in PET degradation (Tournier et al., 2023) and starch hydrolysis (Miłek and Lamkiewicz, 2022). Given that there are no similar materials mentioned in the literature, the enzyme/substrate ratio utilized was almost 80 times lower to what is usually mentioned in low crystallinity PET degradation (Tournier et al., 2023), significantly contributing to the feasibility and viability of the process.

The degradation of prepared mixed (petro-bio)plastic films was determined by analyzing the percentage enzymatic depolymerization of PET-TPS films in comparison to that of neat PET. Post-enzymatic degradation amounts of BHET, MHET, and TPA were determined via HPLC analysis, while the amount of total reducing sugars released in the reaction medium was monitored using the DNS method. Finally, the synergism between LCC^{ICCG} and AMY was calculated to further examine the performance of the combined enzymatic treatment in the biodegradation of mixed PET-TPS materials. LCC^{ICCG} has a known optimal temperature at around 70 °C (Tournier et al., 2020), while AMY shows a wide temperature range from 20 to 70 °C (Tomasik and Horton, 2012). Here, we sought to investigate the impact of the temperature on the synergistic effect of LCC^{ICCG}/AMY to convert mixed PET-TPS plastics into their basic building blocks by performing degradation tests at three different temperatures, *i.e.* 30, 50, and 70 °C. The degradation studies at 30 and 50 °C are discussed in details in Texts S10–S12, Figs. S7–8, supplementary data.

The enzymatic degradation of the mixed PET-TPS films treated with AMY, LCC^{ICCG}, and LCC^{ICCG}/AMY was assessed at 70 °C. It was clear that this temperature exhibited the best overall biodegradation results in our study (Fig. 4), which correlated to improved enzymatic activity for both enzymes at temperatures exceeding 60 °C (Ruiz et al., 2011; Tournier et al., 2020). As expected, LCC^{ICCG} alone showed an improved performance of 53.5 ± 0.1 % enzymatic decomposition for neat PET film at 70 °C. Similarly, this enzyme increased the degradation of the mixed PET-TPS films from around 19 % at 50 °C up to 32 % at 70 °C, as depicted in Fig. 4a. Most importantly, the synergistic action of LCC^{ICCG}/AMY was evident at 70 °C, at which a significant improvement in depolymerization was noted for all mixed PET-TPS samples. The combined LCC^{ICCG}/AMY action remarkably increased enzymatic

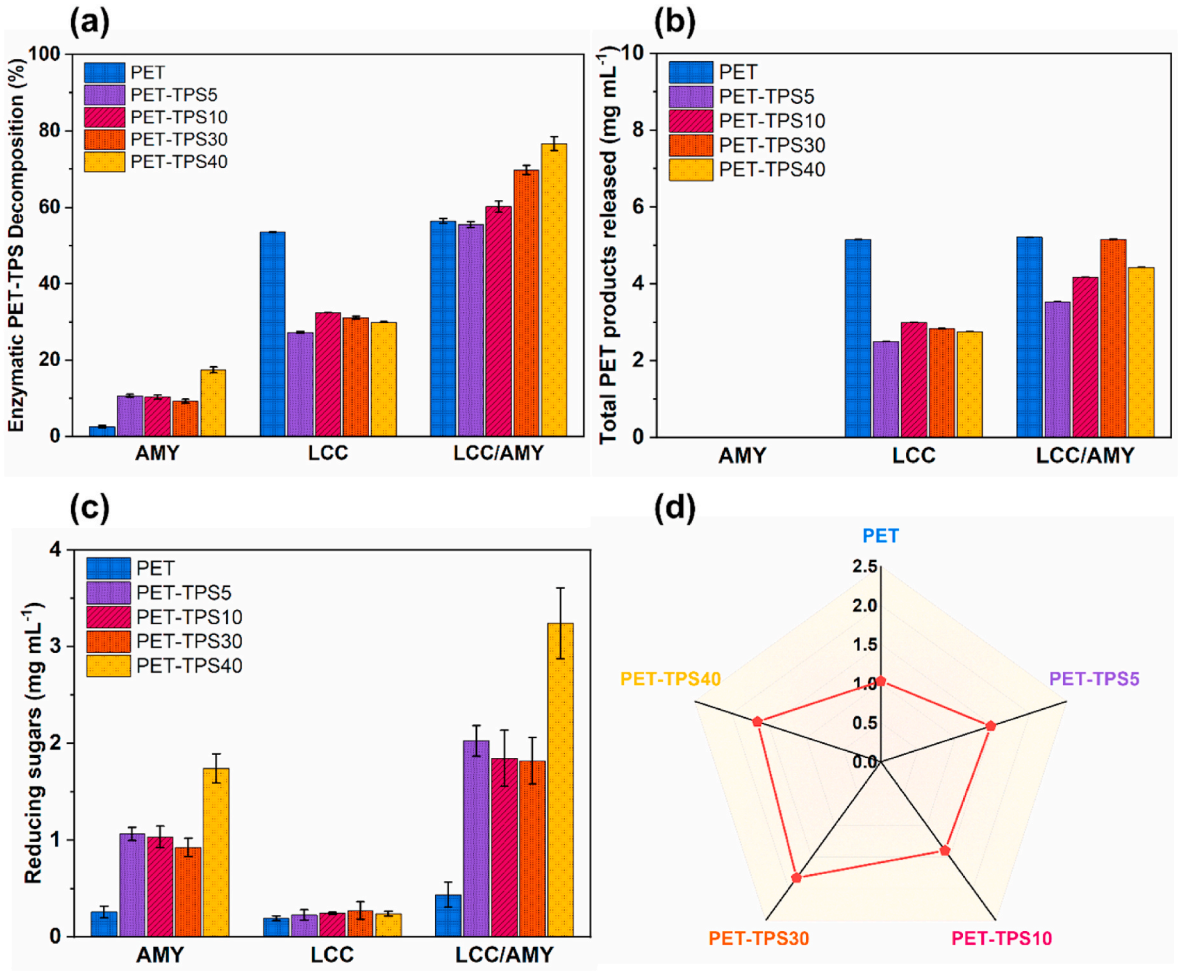

Fig. 4. Enzymatic degradation study on the mixed PET-TPS films using AMY, LCC^{ICCG}, and LCC^{ICCG}/AMY at 70 °C: (a) Enzymatic decomposition (%) calculated from the total degradation products (BHET, MHET, TPA, and reducing sugars); (b) Total PET products released detected by HPLC analysis; (c) Reducing sugars detected via DNS method; and (d) Comparison of DS for the different mixed PET-TPS samples. The concentration of 100 % PET-TPS degradation products is equivalent to 10 mg mL^{-1}. Tests were carried out in triplicate; error bars represent the standard deviation of the mean values.

decomposition percentages to 56, 60, 70, and 77 % for the mixed PET-TPS5, PET-TPS10, PET-TPS30, and PET-TPS40 materials, respectively. Compared to the LCC^{ICCG} single treatment, the LCC^{ICCG}/AMY synergistic action exhibited a 2.0-, 1.9-, 2.2-, and 2.6-fold increase in enzymatic decomposition. Thus, this was a clear evidence of the synergism promoted by the dual-enzyme preparation on the depolymerization of the mixed (petro-bio)plastic samples. Moreover, this exceptional overall performance was attributed to a noteworthy boost observed for degradation products released during the hydrolysis reaction deriving from both PET and TPS counterparts in the mixed (petro-bio)plastic materials.

The detection of total PET intermediate products (TPA, MHET, and BHET) is shown in Fig. 4b. It is worth mentioning that EG is another commonly expected degradation product when TPA is detected, however the HPLC protocol used in this work is not suitable for quantifying EG. AMY does not degrade PET, so no release of TPA, MHET or BHET was observed. It can be noted that the PET degradation products released from the neat PET film remained practically the same after both LCC^{ICCG} and LCC^{ICCG}/AMY treatments at around 5.2 mg mL^{-1}, which was equivalent to a 56 % PET conversion. However, it is evident that the presence of this enzyme in the LCC^{ICCG}/AMY treatment had an important role in synergistically increasing the total mixed PET-TPS film conversion. The addition of AMY to the LCC^{ICCG} enzyme led to an increase in the total amount of reducing sugars (Fig. 4c).

As expected, the amount of total reducing sugars detected for the mixed PET-TPS40 film after enzymatic treatment with AMY at 70 °C increased to 1.74 ± 0.1 mg mL^{-1}. Notably, when PET-TPS40 was treated with LCC^{ICCG}/AMY, the amount of total reducing sugars surged to 3.24 ± 0.3 mg mL^{-1}, a highest in the extent of saccharification among all enzymatic treatments. The identification of reducing sugars provides insights into the simultaneous degradation of the mixed PET-TPS materials, and proves that the synergistic action of these enzymes is of vital importance in order to achieve higher degradation yields. Regarding DS of LCC^{ICCG}/AMY at 70 °C, it varied from 1.4 to 1.8, with the highest value observed in the case of PET-TPS30 (Fig. 4d). It is worth noting that the DS does not appear to be influenced by the temperature, with similar values observed at 30 (Fig. S7d, supplementary data) and 50 °C (Fig. S8d, supplementary data). However, the overall enzymatic depolymerization showed a strong correlation with the reaction temperature change, indicating optimal enzymatic activity of LCC^{ICCG}/AMY at 70 °C. These results emphasize the significance of utilizing enzymatic combinations to enhance the recovery of depolymerization products from mixed (petro-bio)plastic waste, which could then be used as low-cost starting materials for the sustainable production of new synthetic or bio-based polymers.

The yield of PET intermediates TPA, MHET, and BHET resulting from the enzymatic degradation of the neat PET and mixed PET-TPS films was examined at 50 and 70 °C (Fig. 5). The total amount of detected products at 30 °C was approximately 200- and 500-times lower than at 50 and 70 °C, respectively, thus it was intentionally neglected in the interest of calculating the yield of hydrolysis products. TPA was the main PET degradation product for all mixed PET-TPS samples treated by LCC^{ICCG}, from which between 69–100 % and 80–100 % TPA was detected at 50 and 70 °C, respectively (Fig. 5a, c). Interestingly, the treatment of mixed PET-TPS films with LCC^{ICCG}/AMY resulted in slightly higher TPA yields

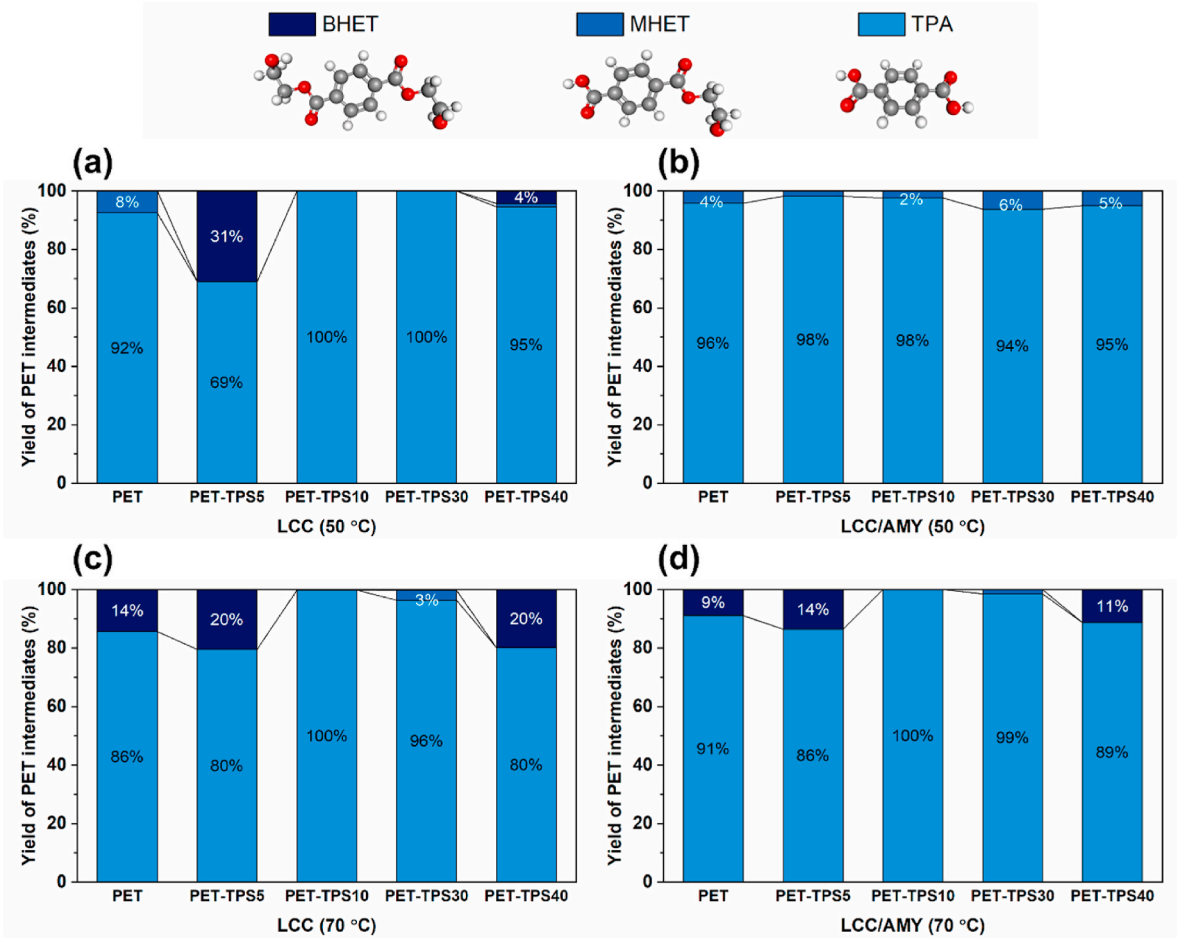

Fig. 5. Yield of PET degradation products (%) detected by HPLC analysis of the neat PET and mixed PET-TPS films: (a) LCC^{ICCG} and (b) LCC^{ICCG}/AMY treatments at 50 °C; (c) LCC^{ICCG} and (d) LCC^{ICCG}/AMY treatments at 70 °C.

in comparison to LCC^{ICCG} alone, from which minimum TPA yields of 94 % (PET-TPS30 at 50 °C, Fig. 5b) and 86 % (PET-TPS5 at 70 °C, Fig. 5d) were measured. Such findings were correlated to the synergistic action of the dual-enzymatic treatment that simultaneously promoted the degradation of the mixed (petro-bio)plastics, where the increased degradation of TPS by AMY enabled the polymer chains of PET to become more easily accessible for the LCC^{ICCG} hydrolytic action, thus increasing the TPA yield.

Further investigation including chemical, thermal, and microstructural analysis assessed the extent of the enzyme-catalyzed depolymerization of the mixed PET-TPS materials and provided a deeper understanding of the hydrolysis reaction. FTIR-ATR was used to enlighten the changes in functional groups of selected PET-TPS40 material compared to that of neat PET films after enzymatic degradation by AMY, LCC^{ICCG}, and LCC^{ICCG}/AMY treatments at 70 °C (Fig. 6). The hydrolytic depolymerization promoted by the enzymatic attack can cleave PET backbone ester bonds and lead to a reduction of carbonyl and subsequent formation of carboxylic and hydroxyl end groups (Brueckner et al., 2008), which contributed to the broad band centered at 1244 cm^{-1}. This agreed with observations reported by Du et al. for PET hydrolysis at 90 °C (Du et al., 2014). This was shown by the shift of the carbonyl ester band from 1712 to 1718 cm^{-1} in the neat PET films treated with LCC^{ICCG} (Fig. 6a–iii) and LCC^{ICCG}/AMY (Fig. 6a–iv), and complete disappearance in the mixed PET-TPS40 film treated with LCC^{ICCG} (Fig. 6b–iii), which confirmed the enzyme ability to degrade PET from the mixed (petro-bio)plastic sample. Donelli et al. have also studied the hydrolysis of PET by cutinase and they observed a similar decrease in the intensity of the carbonyl stretching band associated with the enzymatic attack of PET polymer chains (Donelli et al., 2010). Interestingly, the strong band at 1758 cm^{-1} assigned to the C═O group vibration of TPS could not be detected after the combined LCC^{ICCG}/AMY treatment (Fig. 6b–iv), suggesting the complete decomposition of TPS from the mixed PET-TPS40 waste. Another important aspect to consider, as previously mentioned, is the presence of *trans* and *gauche* rotational conformers of EG in the hydrolyzed materials. As demonstrated in studies by Guo et al. and Wei et al., the conformation of PET oligomer chains simultaneously occurs to varying extents in amorphous (enhanced in *gauche* conformation) and semi-crystalline (enhanced in *trans* conformation) PET materials, and it could be a critical contributor to the enzymatic degradation (Guo et al., 2022; Wei et al., 2019b). The bands at 1471, 1340, 972, and 849 cm^{-1} are associated with the existence of *trans* conformers, whereas *gauche* conformation bands were observed at 1370 and 1044 cm^{-1}, as depicted in Fig. 6a and b. In particular, the spectra of mixed post-enzymatic degradation leftovers from PET-TPS40 treated with LCC^{ICCG} displayed bands enriched in *gauche* conformation, while the LCC^{ICCG}/AMY treatment resulted in enriched *trans* conformation, which suggested the existence of phases predominantly amorphous and crystalline, respectively. In the case of PET, the amorphous regions are considered more susceptible for enzymatic hydrolysis via cleavage of backbone ester bonds (Wei et al., 2019a).

As suggested by the FTIR and DSC results for the mixed PET-TPS films prior to biodegradation studies, the increase of TPS content mixed in PET has resulted in a decrease in the X_c. The reduced crystallinity of the starting PET-TPS films before enzymatic degradation enabled the enhancement of biocatalytic activity (Fig. 4a), resulting in 77 % decomposition of the PET-TPS40 material, which showed the lowest crystallinity value (X_c = 26 %, Table 1), in contrast with a 56 % depolymerization observed for the neat PET film (X_c = 37 %, Table 1), showing a correlation between the mixed materials' low crystallinity and their susceptibility to enzymatic degradation. Upon biocatalytic treatment with LCC^{ICCG}/AMY, noticeable changes in the *CI* and X_c values were observed (Table 2). A rise of up to 5 % in X_c in the neat PET samples treated with AMY or LCC^{ICCG} was noted. In contrast, no significant difference in crystallinity was observed between the non-treated control and that of PET treated with LCC^{ICCG}/AMY. Interestingly, the PET-

Table 2
Properties of the PET and PET-TPS40 materials after enzymatic treatment.

Enzymatic treatment	PET		PET-TPS40	
	CI	X_c (%)	*CI*	X_c (%)
Non-treated	2.6	37.1	3.5	26.0
AMY	3.3	41.4	3.1	27.8
LCC^{ICCG}	2.2	42.5	2.1	24.0
LCC^{ICCG}/AMY	2.7	37.8	1.9	20.7

CI, carbonyl index; X_c, degree of crystallinity.

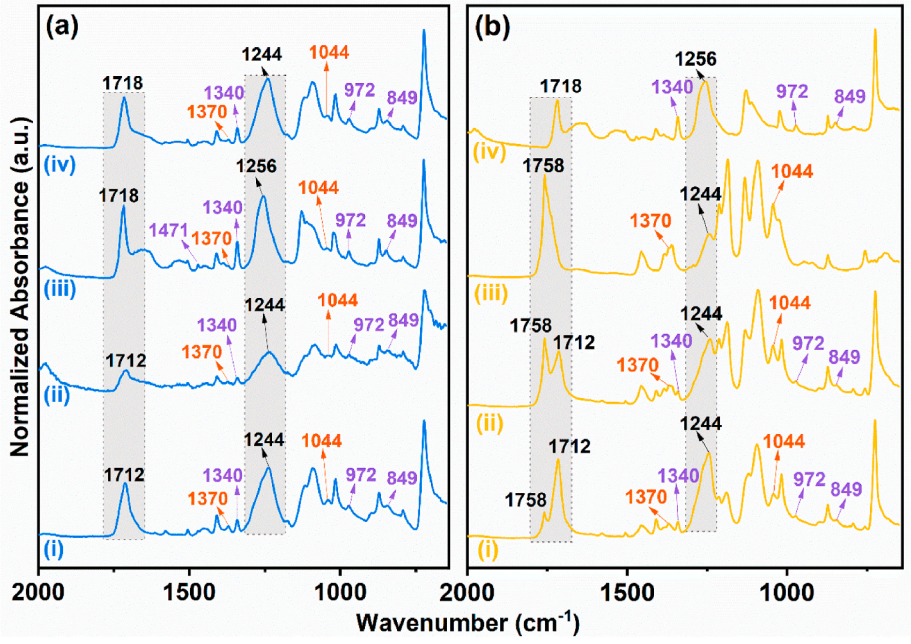

Fig. 6. FTIR spectra of (a) PET and (b) PET-TPS40 films subjected to enzymatic degradation treatments at 70 °C: (i) non-treated control, (ii) AMY, (iii) LCC^{ICCG}, and (iv) LCC^{ICCG}/AMY. Detailed wavenumber range shown: 2000–650 cm^{-1}.

TPS40 film treated with LCC^{ICCG}/AMY showed a −1.25- and −1.84-fold decrease in X_c and *CI* in comparison to those values of non-enzymatically treated samples, respectively. The decrease of the *CI* values was in conformity with the reduction of carbonyl groups, while the reduced X_c value (20.7 %) can be attributed to the LCC^{ICCG}/AMY synergistic effect that simultaneously promote the degradation of amorphous and crystalline regions of the mixed (petro-bio)plastic, which is in agreement with FTIR results.

These results are further confirmed by SEM images of the PET-TPS40 film compared to that of neat PET incubated with LCC^{ICCG}/AMY at 70 °C (Fig. 7). Surface alterations were clearly visible on SEM images of both samples following enzymatic treatment (Fig. 7a', b'). Nonetheless, it can be seen that the synergistic enzymatic surface erosion produced more pronounced cracks on the surface of the PET-TPS40 material compared to the treated neat PET sample. Surface morphology observations recorded by SEM corroborated with the deterioration of thermo-mechanical properties, total release of degradation products, changes in functional groups, and crystallinity of the samples to provide substantial evidence of the synergistic action of the LCC^{ICCG}/AMY enzymes to degrade the studied mixed (petro-bio)plastic waste. Outside bottle-to-bottle mechanical recycling, the majority of post-consumer PET materials, which generally are layered with other petroleum- or bio-based plastics, are still incinerated, accumulated in landfills and oceans, or in the optimal case, mechanically recycled to be used in lower-grade applications. The exploitation of commercial enzymes in enzyme-catalyzed hydrolysis of PET has been well investigated (Brackmann et al., 2023; Carniel et al., 2017; Kim et al., 2021). Here, our findings demonstrate the potential of synergy-promoted enzymatic treatment as a viable bioremediation strategy for treating low-grade mixed (petro--bio)plastic waste. TPA, as the main degradation product, can be isolated and further re-polymerized producing good quality PET that is comparable to virgin resin (Bardoquillo et al., 2023), or alternatively used as feedstock for bacterial production of high-value biodegradable polymers, such as BNC (Esmail et al., 2022) and polyhydroxyalkanoate (PHA) (Kenny et al., 2008). Therefore, this approach holds significant potential in the development of a sustainable and circular economy as it can minimize the environmental impact associated with mixed plastic waste.

3.3. Bio-upcycling of degraded mixed (petro-bio)plastics into bacterial nanocellulose (BNC)

The final part of our work focused on the valorization of post-enzymatic PET-TPS residues into high added-value BNC as an alternative route to manage EoL mixed (petro-bio)plastic waste in a more sustainable way. BNC is a versatile biopolymer with intrinsic physical properties leading to its expansive potential in the broad-spectrum of applications. More specifically, BNC is a generally recognized as safe (GRAS) material by the United States Food and Drug Administration (FDA) with potential applications in the food (Azeredo et al., 2019), low-cost active packaging (Sharma et al., 2021), biomedical (Wahid et al., 2021), and cosmetic (Ludwicka et al., 2016) sectors. To prove our mixed plastic valorization concept, the ability of *K. medellinensis* ID13488 to grow and produce BNC was assessed on liquid residues that

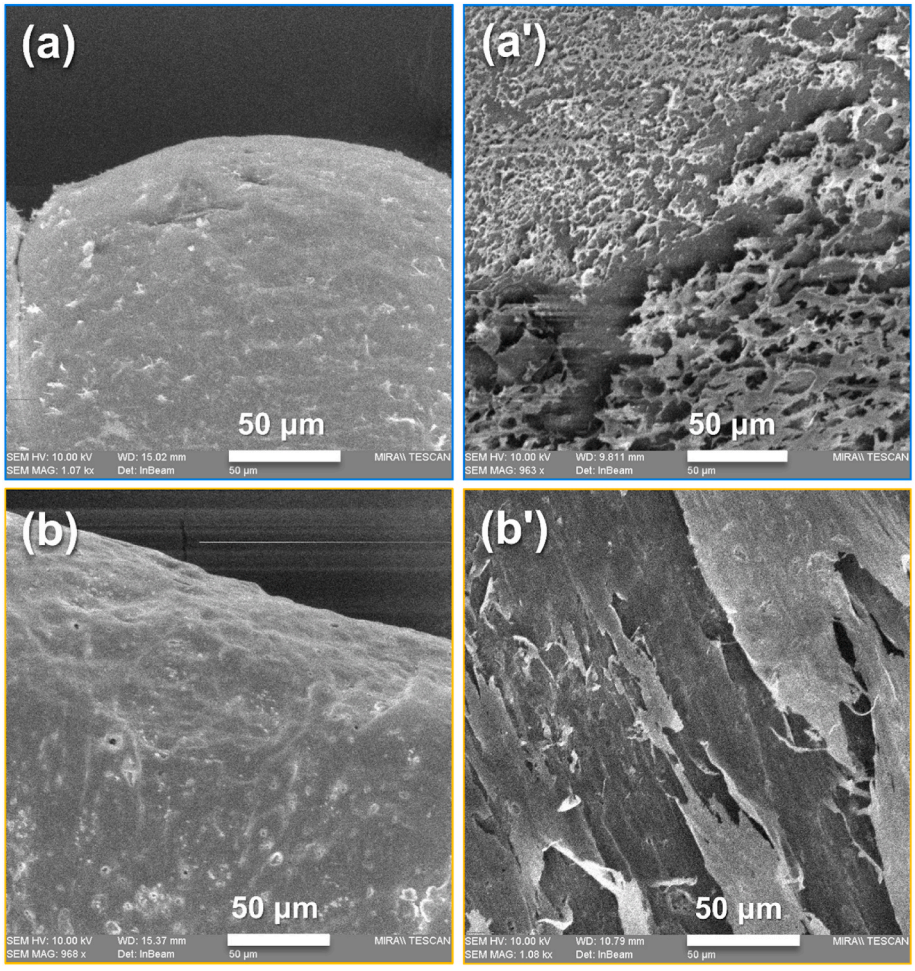

Fig. 7. SEM micrographs of (a) non-treated PET and (b) non-treated PET-TPS40 films in comparison to (a') post-treated PET and (b') post-treated PET-TPS40 samples enzymatically degraded with LCC^{ICCG}/AMY at 70 °C (magnification: 1kx).

remained after degradation of mixed PET-TPS powder samples using AMY, LCC^{ICCG}, and LCC^{ICCG}/AMY after their promising performance on samples in film form. The amount of dry BNC obtained after a ten-day incubation in post-enzymatic liquid residues is presented in Fig. 8a. Compared to the individual AMY and LCC^{ICCG} treatments, the LCC^{ICCG}/AMY treatment resulted in the highest BNC yields harvested after 10 days.

Notably, the synergistic action of the LCC^{ICCG}/AMY treatment that resulted in the highest enzymatic decomposition of the PET-TPS40 material (Fig. 4) was also observed in the yield of BNC (2.9 ± 0.1 g L^{-1}), which recorded a 1.4- and 1.7-fold increase in contrast with the BNC produced from the AMY and LCC^{ICCG} treatments, respectively (Fig. 8a). Despite the fact that the overall conversion rate of PET-TPS40 to BNC was only 0.58 % (Table S2, supplementary data), the significance of this process lies in the considerable increase in the value of the final product. This is due to the substantial difference in prices between PET, ranging up to $1.10/kg, and BNC, which can range from approximately $10/kg to thousands of $/kg (Penloglou et al., 2023; Singh et al., 2021).

The dried BNC obtained from the PET-TPS40 hydrolysates treated with LCC^{ICCG}/AMY was visually and spectroscopically (Molina-Ramírez et al., 2018; Rozenberga et al., 2016) correlated to the BNC grown in HS control medium (Fig. S9, supplementary data). In comparison, Esmail et al. reported the bioconversion of PET degradation products into BNC by *Komagataeibacter xylinus* strains DSM 2004 and DSM 46604, where a 2.1 ± 0.2 g L^{-1} production was the highest yield for *K. xylinus* DSM 2004 strain (Esmail et al., 2022), however, this study used glucose-supplemented medium for the production of BNC, which would still impose excessively high production costs. To further investigate the bioconversion of the mixed (petro-bio)plastic degradation products into BNC, the consumption of reducing sugars was monitored before and after BNC production (Fig. 8b). In particular, 73 % of the sugars obtained from the mixed PET-TPS40 residues after the LCC^{ICCG}/AMY treatment was consumed by *K. medellinensis* during the BNC production. This analysis clearly indicated that sugars released during the enzymatic degradation of the mixed PET-TPS materials were partially utilized for BNC production by the *K. medellinensis* strain. Therefore, this study demonstrates the possibility of using enzymatically degraded mixed (petro-bio)plastic waste as a low-cost feedstock to substitute commercial glucose-based culture medium as a sole carbon and energy source for the production of BNC.

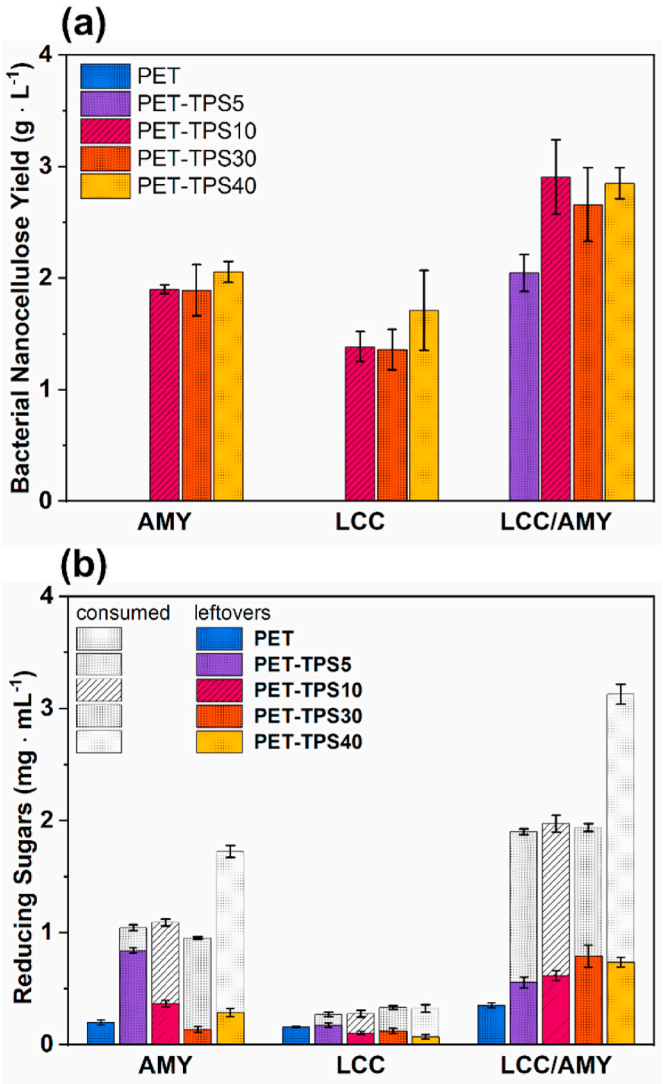

Fig. 8. (a) Bacterial nanocellulose (BNC) yield harvested over a 10-day period using post-enzymatic degradation hydrolysates from the mixed PET-TPS materials treated with AMY, LCC^{ICCG}, and LCC^{ICCG}/AMY treatments; the yield of the control HS medium was 5.5 ± 0.4 g L^{-1} (not shown). (b) Total amount of reducing sugars detected before and after consumption by BNC production.

4. Conclusions

In summary, this study employs enzymes that synergistically degrade plastic waste to deliver biodegradation of mixed (petro-bio)plastic streams and enable bioconversion to high-value products as an EoL management option for plastic waste that is unsustainably incinerated or disposed of in landfills and the environment. The conventional method of PET mechanical recycling employed today cannot address concerns associated with effective waste sorting, leading to contaminated streams and diminished material properties. These PET streams do not meet market specifications, therefore usually end up in landfill, thereby wasting valuable material resources. To model this mixed (petro-bio)plastic waste system, PET was selected as a petroleum-based polymer and TPS as a model bioplastic. PET-TPS materials were prepared via a hot-melt extrusion process. The thermomechanical treatment followed by milling process resulted in lower crystallinity, making the mixed (petro-bio)plastic substrates more attractive for enzymatic depolymerization. These PET-TPS materials were treated using eco-friendly and energy-efficient enzymatic degradation, which employed a combination of LCC^{ICCG} and AMY. Synergistic LCC^{ICCG}/AMY enzymatic activity accounted for a remarkable 77 % decomposition of mixed (petro-bio)plastic (PET-TPS films) into their basic building blocks (mainly TPA and reducing sugars). Moreover, TPA yield measured by HPLC had minimum values of 94 and 86 % in relation to MHET and BHET yields for the LCC^{ICCG}/AMY enzymatic depolymerization at 50 and 70 °C, respectively. Following the effective enzymatic depolymerization, the resulting hydrolysates were then bio-upcycled into added-value BNC films via fermentation, showcasing a circular route to manage mixed (petro-bio)plastic. The highest BNC yield was about 3 g L^{-1} after 10 days of incubation using PET-TPS40 hydrolysates as a low-cost feedstock. Remarkably, even at a low conversion rate of only 0.58 % from PET-TPS plastic to BNC, the proposed biotechnological model holds the potential to valorize low-quality mixed (petro-bio)plastic waste that is currently landfilled to a high-value biomaterial that can cost up to thousands of $/kg. To advance the present concept, future efforts include expanding the use of LCC^{ICCG} in other enzyme combinations as a more sustainable EoL treatment for low-quality mixed (petro-bio)plastic containing other bioplastics such as bio-based polyesters (*e.g.* PCL, PBS, PHB, and PLA) that contaminate petroleum-based waste streams, but also investigating alternative upcycling solutions including production of other biopolymers (*e.g.* PHAs). Across the board, our study opens a new biotechnological route based on synergy-promoted enzymatic degradation and bioconversion of mixed (petro-bio)plastic waste into sustainable eco-polymers towards an attractive circular, bio-based economy for plastics.

CRediT authorship contribution statement

Jeovan A. Araujo: Writing – review & editing, Writing – original draft, Visualization, Validation, Methodology, Investigation, Formal analysis, Conceptualization. **George Taxeidis:** Writing – review & editing, Writing – original draft, Methodology, Investigation, Formal analysis, Conceptualization. **Everton Henrique Da Silva Pereira:** Validation, Investigation. **Muhammad Azeem:** Investigation, Formal analysis. **Brana Pantelic:** Methodology, Investigation. **Sanja Jeremic:** Methodology, Investigation. **Marijana Ponjavic:** Methodology, Investigation. **Yuanyuan Chen:** Investigation. **Marija Mojicevic:** Validation, Project administration, Investigation. **Jasmina Nikodinovic-Runic:** Supervision, Resources, Conceptualization. **Evangelos Topakas:** Supervision, Resources, Conceptualization. **Margaret Brennan Fournet:** Writing – review & editing, Supervision, Funding acquisition.

Declaration of competing interest

The authors declare that they have no known competing financial interests or personal relationships that could have appeared to influence the work reported in this paper.

Data availability

Data will be made available on request.

Acknowledgements

This work was supported by the European Union's Horizon 2020 Research and Innovation program [grant number: 870292 (BioICEP)]. European Union's Horizon Europe EIC Pathfinder program [grant number: 101046758 (EcoPlastiC)]. George Taxeidis was financially supported by the H.F.R.I (Elidek) institution (PhD Scholarship). The authors kindly acknowledge the Applied Polymer Technologies (APT Gateway, TUS Athlone) for providing the facilities for polymer processing, and the Centre for Industrial Services & Design (CISD, TUS Athlone) for supporting with materials characterization. The APT Gateway is co-funded by the Government of Ireland and the European Union through the ERDF Southern, Eastern & Midland Regional Programme 2021–27.

Abbreviations

AMY	commercial amylase
BHET	bis(2-hydroxyethyl) terephthalic acid
BNC	bacterial nanocellulose
CI	carbonyl index
DNS	dinitrosalicylic acid
EG	ethylene glycol
EU	European Union
HPLC	high performance liquid chromatography
IPTG	isopropyl β-D-1-thiogalactopyranoside
LCC^{ICCG}	Leaf-branch compost cutinase
MHET	mono-(2-hydroxyethyl) terephthalic acid
PBS	polybutylene succinate
PCL	polycaprolactone
PET	polyethylene terephthalate
PHAs	polyhydroxyalkanoates
PHB	polyhydroxybutyrate
PLA	polylactic acid
T_g	glass transition temperature
TPA	terephthalic acid
TPS	thermoplastic starch
X_c	degree of crystallinity

Appendix A. Supplementary data

Supplementary data to this article can be found online at https://doi.org/10.1016/j.jclepro.2024.141025.

References

Åkesson, D., Kuzhanthaivelu, G., Bohlén, M., 2021. Effect of a small amount of thermoplastic starch blend on the mechanical recycling of conventional plastics. J. Polym. Environ. 29, 985–991. https://doi.org/10.1007/s10924-020-01933-2.

Ansink, E., Wijk, L., Zuidmeer, F., 2022. No clue about bioplastics. Ecol. Econ. 191, 107245 https://doi.org/10.1016/j.ecolecon.2021.107245.

Araujo, J.A., Cortese, Y.J., Mojicevic, M., Brennan Fournet, M., Chen, Y., 2021. Composite films of thermoplastic starch and CaCl2 extracted from eggshells for extending food shelf-life. Polysaccharides 2, 677–690. https://doi.org/10.3390/polysaccharides2030041.

Azeredo, H.M.C., Barud, H., Farinas, C.S., Vasconcellos, V.M., Claro, A.M., 2019. Bacterial cellulose as a raw material for food and food packaging applications. Front. Sustain. Food Syst. 3, 429319 https://doi.org/10.3389/FSUFS.2019.00007/BIBTEX.

Bardoquillo, E.I.M., Firman, J.M.B., Montecastro, D.B., Basilio, A.M., 2023. Chemical recycling of waste polyethylene terephthalate (PET) bottles via recovery and polymerization of terephthalic acid (TPA) and ethylene glycol (EG). Mater. Today Proc. https://doi.org/10.1016/j.matpr.2023.04.160.

Bergel, B.F., Dias Osorio, S., da Luz, L.M., Santana, R.M.C., 2018. Effects of hydrophobized starches on thermoplastic starch foams made from potato starch. Carbohydr. Polym. 200, 106–114. https://doi.org/10.1016/j.carbpol.2018.07.047.

Borrelle, S.B., Ringma, J., Law, K.L., Monnahan, C.C., Lebreton, L., McGivern, A., Murphy, E., Jambeck, J., Leonard, G.H., Hilleary, M.A., Eriksen, M., Possingham, H. P., De Frond, H., Gerber, L.R., Polidoro, B., Tahir, A., Bernard, M., Mallos, N., Barnes, M., Rochman, C.M., 2020. Predicted growth in plastic waste exceeds efforts to mitigate plastic pollution. Science 369, 1515–1518. https://doi.org/10.1126/science.aba3656, 1979.

Brackmann, R., de Oliveira Veloso, C., de Castro, A.M., Langone, M.A.P., 2023. Enzymatic post-consumer poly(ethylene terephthalate) (PET) depolymerization using commercial enzymes. 3 Biotech 13, 135. https://doi.org/10.1007/s13205-023-03555-6.

Brueckner, T., Eberl, A., Heumann, S., Rabe, M., Guebitz, G.M., 2008. Enzymatic and chemical hydrolysis of poly(ethylene terephthalate) fabrics. J. Polym. Sci. Polym. Chem. 46, 6435–6443. https://doi.org/10.1002/pola.22952.

Carniel, A., Valoni, É., Nicomedes, J., Gomes, A. da C., Castro, A.M. de, 2017. Lipase from Candida Antarctica (CALB) and cutinase from Humicola insolens act synergistically for PET hydrolysis to terephthalic acid. Process Biochem. 59, 84–90. https://doi.org/10.1016/j.procbio.2016.07.023.

Chen, Z., Hay, J.N., Jenkins, M.J., 2012. FTIR spectroscopic analysis of poly(ethylene terephthalate) on crystallization. Eur. Polym. J. 48, 1586–1610. https://doi.org/10.1016/j.eurpolymj.2012.06.006.

Darko, C., Yung, P.W.S., Chen, A., Acquaye, A., 2023. Review and recommendations for sustainable pathways of recycling commodity plastic waste across different economic regions. Resourc. Environ. Sustain. 14, 100134 https://doi.org/10.1016/j.resenv.2023.100134.

Del Mar Castro López, M., Ares Pernas, A.I., Abad López, M.J., Latorre, A.L., López Vilariño, J.M., González Rodríguez, M.V., 2014. Assessing changes on poly(ethylene terephthalate) properties after recycling: mechanical recycling in laboratory versus postconsumer recycled material. Mater. Chem. Phys. 147, 884–894. https://doi.org/10.1016/j.matchemphys.2014.06.034.

Dimarogona, M., Nikolaivits, E., Kanelli, M., Christakopoulos, P., Sandgren, M., Topakas, E., 2015. Structural and functional studies of a Fusarium oxysporum cutinase with polyethylene terephthalate modification potential. Biochim. Biophys. Acta Gen. Subj. 1850, 2308–2317. https://doi.org/10.1016/j.bbagen.2015.08.009.

Diop, C.I.K., Li, H.L., Xie, B.J., Shi, J., 2011. Effects of acetic acid/acetic anhydride ratios on the properties of corn starch acetates. Food Chem. 126, 1662–1669. https://doi.org/10.1016/j.foodchem.2010.12.050.

Donelli, I., Freddi, G., Nierstrasz, V.A., Taddei, P., 2010. Surface structure and properties of poly-(ethylene terephthalate) hydrolyzed by alkali and cutinase. Polym. Degrad. Stabil. 95, 1542–1550. https://doi.org/10.1016/j.polymdegradstab.2010.06.011.

Donelli, I., Taddei, P., Smet, P.F., Poelman, D., Nierstrasz, V.A., Freddi, G., 2009. Enzymatic surface modification and functionalization of PET: a water contact angle, FTIR, and fluorescence spectroscopy study. Biotechnol. Bioeng. 103, 845–856. https://doi.org/10.1002/bit.22316.

Du, B., Yang, R., Xie, X., 2014. Investigation of hydrolysis in poly(ethylene terephthalate) by FTIR-ATR. Chin. J. Polym. Sci. 32, 230–235. https://doi.org/10.1007/s10118-014-1372-6.

Esmail, A., Rebocho, A.T., Marques, A.C., Silvestre, S., Gonçalves, A., Fortunato, E., Torres, C.A.V., Reis, M.A.M., Freitas, F., 2022. Bioconversion of terephthalic acid and ethylene glycol into bacterial cellulose by komagataeibacter xylinus DSM 2004 and DSM 46604. Front. Bioeng. Biotechnol. 10 https://doi.org/10.3389/fbioe.2022.853322.

European Bioplastics Conference, 2021. Bioplastics Market Development Update 2021. Berlin.

Filho, W.L., Salvia, A.L., Bonoli, A., Saari, U.A., Voronova, V., Klõga, M., Kumbhar, S.S., Olszewski, K., De Quevedo, D.M., Barbir, J., 2021. An assessment of attitudes towards plastics and bioplastics in Europe. Sci. Total Environ. 755, 142732 https://doi.org/10.1016/j.scitotenv.2020.142732.

Fotopoulou, K.N., Karapanagioti, H.K., 2017. Degradation of various plastics in the environment. In: Takada, H., Karapanagioti, H.K. (Eds.), The Handbook of Environmental Chemistry. Springer, Cham, pp. 71–92. https://doi.org/10.1007/698_2017_11.

Friedrich, D., 2021. What makes bioplastics innovative for fashion retailers? An in-depth analysis according to the Triple Bottom Line Principle. J. Clean. Prod. 316, 128257 https://doi.org/10.1016/j.jclepro.2021.128257.

Gasteiger, E., Hoogland, C., Gattiker, A., Duvaud, S., Wilkins, M.R., Appel, R.D., Bairoch, A., 2005. Protein identification and analysis tools on the ExPASy server. In: The Proteomics Protocols Handbook. Humana Press, Totowa, NJ, pp. 571–607. https://doi.org/10.1385/1-59259-890-0:571.

Gere, D., Czigany, T., 2018. Rheological and mechanical properties of recycled polyethylene films contaminated by biopolymer. Waste Manag. 76, 190–198. https://doi.org/10.1016/j.wasman.2018.02.045.

Geyer, R., Jambeck, J.R., Law, K.L., 2017. Production, use, and fate of all plastics ever made. Sci. Adv. 3 https://doi.org/10.1126/sciadv.1700782.

Gioia, C., Giacobazzi, G., Vannini, M., Totaro, G., Sisti, L., Colonna, M., Marchese, P., Celli, A., 2021. End of life of biodegradable plastics: composting versus Re/upcycling. ChemSusChem 14, 4167–4175. https://doi.org/10.1002/cssc.202101226.

Grant, A., Bapasola, A., von Eye, M., Cordle, M., Dionisi, F., Loo, S., 2023. Mixed Waste Sorting to Meet the EU's Circular Economy Objectives. Bristol.

Guo, B., Vanga, S.R., Lopez-Lorenzo, X., Saenz-Mendez, P., Ericsson, S.R., Fang, Y., Ye, X., Schriever, K., Bäckström, E., Biundo, A., Zubarev, R.A., Furó, I., Hakkarainen, M., Syrén, P.-O., 2022. Conformational selection in biocatalytic plastic degradation by PETase. ACS Catal. 12, 3397–3409. https://doi.org/10.1021/acscatal.1c05548.

Jozala, A.F., de Lencastre-Novaes, L.C., Lopes, A.M., de Carvalho Santos-Ebinuma, V., Mazzola, P.G., Pessoa-Jr, A., Grotto, D., Gerenutti, M., Chaud, M.V., 2016. Bacterial nanocellulose production and application: a 10-year overview. Appl. Microbiol. Biotechnol. 100, 2063–2072. https://doi.org/10.1007/s00253-015-7243-4.

Kenny, S.T., Runic, J.N., Kaminsky, W., Woods, T., Babu, R.P., Keely, C.M., Blau, W., O'Connor, K.E., 2008. Up-cycling of PET (polyethylene terephthalate) to the biodegradable plastic PHA (polyhydroxyalkanoate). Environ. Sci. Technol. 42, 7696–7701. https://doi.org/10.1021/es801010e.

Kim, D.H., Han, D.O., Shim, K., Kim, J.K., Pelton, J.G., Ryu, M.H., Joo, J.C., Han, J.W., Kim, H.T., Kim, K.H., 2021. One-pot chemo-bioprocess of PET depolymerization and recycling enabled by a biocompatible catalyst, betaine. ACS Catal. 11, 3996–4008. https://doi.org/10.1021/acscatal.0c04014.

Kim, N.K., Lee, S.H., Park, H.D., 2022. Current biotechnologies on depolymerization of polyethylene terephthalate (PET) and repolymerization of reclaimed monomers from PET for bio-upcycling: a critical review. Bioresour. Technol. 363, 127931 https://doi.org/10.1016/J.BIORTECH.2022.127931.

Kourmentza, C., Plácido, J., Venetsaneas, N., Burniol-Figols, A., Varrone, C., Gavala, H. N., Reis, M.A.M., 2017. Recent advances and challenges towards sustainable polyhydroxyalkanoate (PHA) production. Bioengineering 4, 55. https://doi.org/10.3390/bioengineering4020055.

Kulas, D.G., Zolghadr, A., Chaudhari, U.S., Shonnard, D.R., 2023. Economic and environmental analysis of plastics pyrolysis after secondary sortation of mixed plastic waste. J. Clean. Prod. 384, 135542 https://doi.org/10.1016/j.jclepro.2022.135542.

Lee, S., Lee, Y.R., Kim, S.J., Lee, J.-S., Min, K., 2023. Recent advances and challenges in the biotechnological upcycling of plastic wastes for constructing a circular bioeconomy. Chem. Eng. J. 454, 140470 https://doi.org/10.1016/j.cej.2022.140470.

Ludwicka, K., Jedrzejczak-Krzepkowska, M., Kubiak, K., Kolodziejczyk, M., Pankiewicz, T., Bielecki, S., 2016. Medical and cosmetic applications of bacterial NanoCellulose. Bacter. Nanocell.: Biotechnol. Bio-Econ. 145–165. https://doi.org/10.1016/B978-0-444-63458-0.00009-3.

Makryniotis, K., Nikolaivits, E., Gkountela, C., Vouyiouka, S., Topakas, E., 2023. Discovery of a polyesterase from Deinococcus maricopensis and comparison to the benchmark LCCICCG suggests high potential for semi-crystalline post-consumer PET degradation. J. Hazard Mater. 455, 131574 https://doi.org/10.1016/j.jhazmat.2023.131574.

Miłek, J., Lamkiewicz, J., 2022. The starch hydrolysis by α-amylase Bacillus spp.: an estimation of the optimum temperatures, the activation and deactivation energies. J. Therm. Anal. Calorim. 147, 14459–14466. https://doi.org/10.1007/S10973-022-11738-1/TABLES/3.

Miller, G.L., 1959. Use of dinitrosalicylic acid reagent for determination of reducing sugar. Anal. Chem. 31, 426–428. https://doi.org/10.1021/ac60147a030.

Molina-Ramírez, C., Enciso, C., Torres-Taborda, M., Zuluaga, R., Gañán, P., Rojas, O.J., Castro, C., 2018. Effects of alternative energy sources on bacterial cellulose characteristics produced by Komagataeibacter medellinensis. Int. J. Biol. Macromol. 117, 735–741. https://doi.org/10.1016/j.ijbiomac.2018.05.195.

Muhammad Shamsuddin, I., 2017. Bioplastics as better alternative to petroplastics and their role in national sustainability: a review. Adv. Biosci. Bioeng. 5, 63. https://doi.org/10.11648/j.abb.20170504.13.

Narancic, T., Verstichel, S., Reddy Chaganti, S., Morales-Gamez, L., Kenny, S.T., De Wilde, B., Babu Padamati, R., O'Connor, K.E., 2018. Biodegradable plastic blends create new possibilities for end-of-life management of plastics but they are not a panacea for plastic pollution. Environ. Sci. Technol. 52, 10441–10452. https://doi.org/10.1021/acs.est.8b02963.

Navya, P.V., Gayathri, V., Samanta, D., Sampath, S., 2022. Bacterial cellulose: a promising biopolymer with interesting properties and applications. Int. J. Biol. Macromol. 220, 435–461. https://doi.org/10.1016/j.ijbiomac.2022.08.056.

Nikolaivits, E., Taxeidis, G., Gkountela, C., Vouyiouka, S., Maslak, V., Nikodinovic-Runic, J., Topakas, E., 2022. A polyesterase from the Antarctic bacterium Moraxella sp. degrades highly crystalline synthetic polymers. J. Hazard Mater. 434, 128900 https://doi.org/10.1016/j.jhazmat.2022.128900.

Pantelic, B., Araujo, J.A., Jeremic, S., Azeem, M., Attallah, O.A., Slaperas, R., Mojicevic, M., Chen, Y., Fournet, M.B., Topakas, E., Nikodinovic-Runic, J., 2023. A novel Bacillus subtilis BPM12 with high bis(2 hydroxyethyl)terephthalate hydrolytic activity efficiently interacts with virgin and mechanically recycled polyethylene terephthalate. Environ. Technol. Innov., 103316 https://doi.org/10.1016/j.eti.2023.103316.

Pantelic, B., Ponjavic, M., Jankovic, V., Aleksic, I., Stevanovic, S., Murray, J., Fournet, M. B., Nikodinovic-Runic, J., 2021. Upcycling biodegradable PVA/starch film to a bacterial biopigment and biopolymer. Polymers 13, 3692. https://doi.org/10.3390/polym13213692.

Patel, A., Chang, A.C., Mastromonaco, A., Acosta Diaz, M., Perry, S., Ferki, O., Ayafor, C., Abid, U., Wong, H.-W., Xie, D., Sobkowicz, M.J., 2023. Aqueous buffer solution-induced crystallization competes with enzymatic depolymerization of pre-treated post-consumer poly (ethylene terephthalate) waste. Polymer (Guildf) 285, 126370. https://doi.org/10.1016/j.polymer.2023.126370.

Patel, A., Chang, A.C., Perry, S., Soong, Y.-H.V., Ayafor, C., Wong, H.-W., Xie, D., Sobkowicz, M.J., 2022. Melt processing pretreatment effects on enzymatic depolymerization of poly(ethylene terephthalate). ACS Sustain. Chem. Eng. 10, 13619–13628. https://doi.org/10.1021/acssuschemeng.2c03142.

Penloglou, G., Basna, A., Pavlou, A., Kiparissides, C., 2023. Techno-economic considerations on nanocellulose's future progress: a short review. Processes 11, 2312. https://doi.org/10.3390/pr11082312.

Quecholac-Piña, X., García-Rivera, M.A., Espinosa-Valdemar, R.M., Vázquez-Morillas, A., Beltrán-Villavicencio, M., Cisneros-Ramos, A. de la L., 2017. Biodegradation of compostable and oxodegradable plastic films by backyard composting and bioaugmentation. Environ. Sci. Pollut. Control Ser. 24, 25725–25730. https://doi.org/10.1007/s11356-016-6553-0.

Rochman, C.M., Browne, M.A., Halpern, B.S., Hentschel, B.T., Hoh, E., Karapanagioti, H. K., Rios-Mendoza, L.M., Takada, H., Teh, S., Thompson, R.C., 2013. Classify plastic waste as hazardous. Nature 494, 169–171. https://doi.org/10.1038/494169a.

Rosenboom, J.-G., Langer, R., Traverso, G., 2022. Bioplastics for a circular economy. Nat. Rev. Mater. 7, 117–137. https://doi.org/10.1038/s41578-021-00407-8.

Rozenberga, L., Skute, M., Belkova, L., Sable, I., Vikele, L., Semjonovs, P., Saka, M., Ruklisha, M., Paegle, L., 2016. Characterisation of films and nanopaper obtained from cellulose synthesised by acetic acid bacteria. Carbohydr. Polym. 144, 33–40. https://doi.org/10.1016/j.carbpol.2016.02.025.

Ruiz, M.I., Sanchez, C.I., Torrres, R.G., Molina, D.R., 2011. Enzymatic hydrolysis of cassava starch for production of bioethanol with a colombian wild yeast strain. J. Braz. Chem. Soc. 22, 2337–2343. https://doi.org/10.1590/S0103-50532011001200014.

Sammon, C., Yarwood, J., Everall, N., 2000. An FTIR Study of the Effect of Hydrolytic Degradation on the Structure of Thin PET Films. Polym Degrad Stab 67, 149–158. https://doi.org/10.1016/S0141-3910(99)00104-4.

Schyns, Z.O.G., Shaver, M.P., 2021. Mechanical recycling of packaging plastics: a review. Macromol. Rapid Commun. 42 https://doi.org/10.1002/marc.202000415.

Shafqat, A., Tahir, A., Mahmood, A., Tabinda, A.B., Yasar, A., Pugazhendhi, A., 2020. A review on environmental significance carbon foot prints of starch based bio-plastic: a substitute of conventional plastics. Biocatal. Agric. Biotechnol. 27, 101540 https://doi.org/10.1016/J.BCAB.2020.101540.

Sharma, C., Bhardwaj, N.K., Pathak, P., 2021. Static intermittent fed-batch production of bacterial nanocellulose from black tea and its modification using chitosan to develop antibacterial green packaging material. J. Clean. Prod. 279, 123608 https://doi.org/10.1016/j.jclepro.2020.123608.

Siddiqui, M.N., Redhwi, H.H., Al-Arfaj, A.A., Achilias, D.S., 2021. Chemical recycling of PET in the presence of the bio-based polymers, PLA, PHB and PEF: a review. Sustainability 13, 10528. https://doi.org/10.3390/su131910528.

Singh, A., Rorrer, N.A., Nicholson, S.R., Erickson, E., DesVeaux, J.S., Avelino, A.F.T., Lamers, P., Bhatt, A., Zhang, Y., Avery, G., Tao, L., Pickford, A.R., Carpenter, A.C., McGeehan, J.E., Beckham, G.T., 2021. Techno-economic, life-cycle, and socioeconomic impact analysis of enzymatic recycling of poly(ethylene terephthalate). Joule 5, 2479–2503. https://doi.org/10.1016/j.joule.2021.06.015.

Sintawee, S., Saya, Y., Eiko, K., Joong-Jae, K., Yuichi, K., Kazufumi, T., Shigenori, K., 2012. Isolation of a novel cutinase homolog with polyethylene terephthalate-degrading activity from leaf-branch compost by using a metagenomic approach. Appl. Environ. Microbiol. 78, 1556–1562. https://doi.org/10.1128/AEM.06725-11.

Soong, Y.-H.V., Sobkowicz, M.J., Xie, D., 2022. Recent advances in biological recycling of polyethylene terephthalate (PET) plastic wastes. Bioengineering 9, 98. https://doi.org/10.3390/bioengineering9030098.

Sullivan, K.P., Werner, A.Z., Ramirez, K.J., Ellis, L.D., Bussard, J.R., Black, B.A., Brandner, D.G., Bratti, F., Buss, B.L., Dong, X., Haugen, S.J., Ingraham, M.A., Konev, M.O., Michener, W.E., Miscall, J., Pardo, I., Woodworth, S.P., Guss, A.M., Román-Leshkov, Y., Stahl, S.S., Beckham, G.T., 2022. Mixed plastics waste valorization through tandem chemical oxidation and biological funneling. Science 378, 207–211. https://doi.org/10.1126/science.abo4626.

Thiounn, T., Smith, R.C., 2020. Advances and approaches for chemical recycling of plastic waste. J. Polym. Sci. 58, 1347–1364. https://doi.org/10.1002/POL.20190261.

Thomsen, T.B., Hunt, C.J., Meyer, A.S., 2022. Influence of substrate crystallinity and glass transition temperature on enzymatic degradation of polyethylene terephthalate (PET). Nat. Biotechnol. 69, 28–35. https://doi.org/10.1016/J.NBT.2022.02.006.

Tomasik, P., Horton, D., 2012. Enzymatic conversions of starch. In: Advances in Carbohydrate Chemistry and Biochemistry. Elsevier, pp. 59–436. https://doi.org/10.1016/B978-0-12-396523-3.00001-4.

Tournier, V., Duquesne, S., Guillamot, F., Cramail, H., Taton, D., Marty, A., André, I., 2023. Enzymes' power for plastics degradation. Chem. Rev. 123, 5612–5701. https://doi.org/10.1021/acs.chemrev.2c00644.

Tournier, V., Topham, C.M., Gilles, A., David, B., Folgoas, C., Moya-Leclair, E., Kamionka, E., Desrousseaux, M.-L., Texier, H., Gavalda, S., Cot, M., Guémard, E., Dalibey, M., Nomme, J., Cioci, G., Barbe, S., Chateau, M., André, I., Duquesne, S., Marty, A., 2020. An engineered PET depolymerase to break down and recycle plastic bottles. Nature 580, 216–219. https://doi.org/10.1038/s41586-020-2149-4.

von Haugwitz, G., Han, X., Pfaff, L., Li, Q., Wei, H., Gao, J., Methling, K., Ao, Y., Brack, Y., Mican, J., Feiler, C.G., Weiss, M.S., Bednar, D., Palm, G.J., Lalk, M., Lammers, M., Damborsky, J., Weber, G., Liu, W., Bornscheuer, U.T., Wei, R., 2022. Structural insights into (Tere)phthalate-Ester hydrolysis by a carboxylesterase and its role in promoting PET depolymerization. ACS Catal. 12, 15259–15270. https://doi.org/10.1021/acscatal.2c03772.

Wahid, F., Huang, L.-H., Zhao, X.-Q., Li, W.-C., Wang, Y.-Y., Jia, S.-R., Zhong, C., 2021. Bacterial cellulose and its potential for biomedical applications. Biotechnol. Adv. 53, 107856 https://doi.org/10.1016/j.biotechadv.2021.107856.

Wang, L., Bank, M.S., Rinklebe, J., Hou, D., 2023. Plastic–rock complexes as hotspots for microplastic generation. Environ. Sci. Technol. 57, 7009–7017. https://doi.org/10.1021/acs.est.3c00662.

Wei, R., Breite, D., Song, C., Gräsing, D., Ploss, T., Hille, P., Schwerdtfeger, R., Matysik, J., Schulze, A., Zimmermann, W., 2019a. Biocatalytic degradation efficiency of postconsumer polyethylene terephthalate packaging determined by their polymer microstructures. Adv. Sci. 6 https://doi.org/10.1002/advs.201900491.

Wei, R., Song, C., Gräsing, D., Schneider, T., Bielytskyi, P., Böttcher, D., Matysik, J., Bornscheuer, U.T., Zimmermann, W., 2019b. Conformational fitting of a flexible oligomeric substrate does not explain the enzymatic PET degradation. Nat. Commun. 10, 5581. https://doi.org/10.1038/s41467-019-13492-9.

Wunderlich, B., 1973. In: Wunderlich, B.B.T.-M.P. (Ed.), CHAPTER III - the Crystal Morphology. Academic Press, pp. 178–379. https://doi.org/10.1016/B978-0-12-765601-4.50008-1.

Yang, S.-S., Wu, W.-M., Pang, J.-W., He, L., Ding, M.-Q., Li, M.-X., Zhao, Y.-L., Sun, H.-J., Xing, D.-F., Ren, N.-Q., Yang, J., Criddle, C.S., Ding, J., 2023. Bibliometric analysis of publications on biodegradation of plastics: explosively emerging research over 70 years. J. Clean. Prod., 139423 https://doi.org/10.1016/j.jclepro.2023.139423.

Yoshida, S., Hiraga, K., Takehana, T., Taniguchi, I., Yamaji, H., Maeda, Y., Toyohara, K., Miyamoto, K., Kimura, Y., Oda, K., 2016. A bacterium that degrades and assimilates poly(ethylene terephthalate). Science 351, 1196–1199. https://doi.org/10.1126/science.aad6359, 1979.

Zekriardehani, S., Jabarin, S.A., Gidley, D.R., Coleman, M.R., 2017. Effect of chain dynamics, crystallinity, and free volume on the barrier properties of poly(ethylene terephthalate) biaxially oriented films. Macromolecules 50, 2845–2855. https://doi.org/10.1021/acs.macromol.7b00198.

Zhu, B., Wang, D., Wei, N., 2022. Enzyme discovery and engineering for sustainable plastic recycling. Trends Biotechnol. 40, 22–37. https://doi.org/10.1016/J.TIBTECH.2021.02.008.